Monterey(!) Petroleum System of the Onshore Santa Maria Basin

Road Log

Arrival	Departure	Cum. Miles	Stop #	Stop Description	Special Notes/Hazards
7:30 a.m.	8:00 a.m.		0	Embassy Suites parking lot	Leave on time. Restroom stop.
8:15 a.m.	9:30 a.m.	4.4	1	Sweeney Road	No restroom. Use orange safety vests. Beware of road traffic.
10:00 a.m.	10:45 a.m.	16.6	2	Vandenberg Air Force Base	Check-in can take a long time. Restroom stop.
10:45 a.m.	Noon	23.9	3	Lompoc Landing	Beware of rocky terrain/unsure footing and waves.
12:15 p.m.	1:15 p.m.	25.5	4	Lunch on beach	Observe cordoned off area, if present. Porta potty available.
2:00 p.m.	3:30 p.m.	43.1	5	Lions Head	Beware of rocky terrain/unsure footing and waves. Restroom at base exit if needed.
4:30/5:00 p.m.		66.0	0	Embassy Suites parking lot	Time to relax.

Sunrise: 6:37 a.m. Sunset: 4:58 p.m.
Low tide: 0.3 at 2:15 p.m. High tide: 5.4 at 7:40 a.m.

This field guide is organized as follows:

All photos are by Allegra Hosford Scheirer (allegras@stanford.edu) and Les Magoon (lmagoon@sgtanford.edu) unless otherwise noted. This field guide is for internal use only and is not to be published or used by others without permission.

Stop 0: Embassy Suites by Hilton Central Coast parking lot, Lompoc, CA
-120.4587° 34.6559°

Stop 1: Sweeney Road, Lompoc, CA
-120.4085° 34.6415°
Mapquest map from hotel to Sweeney Rd

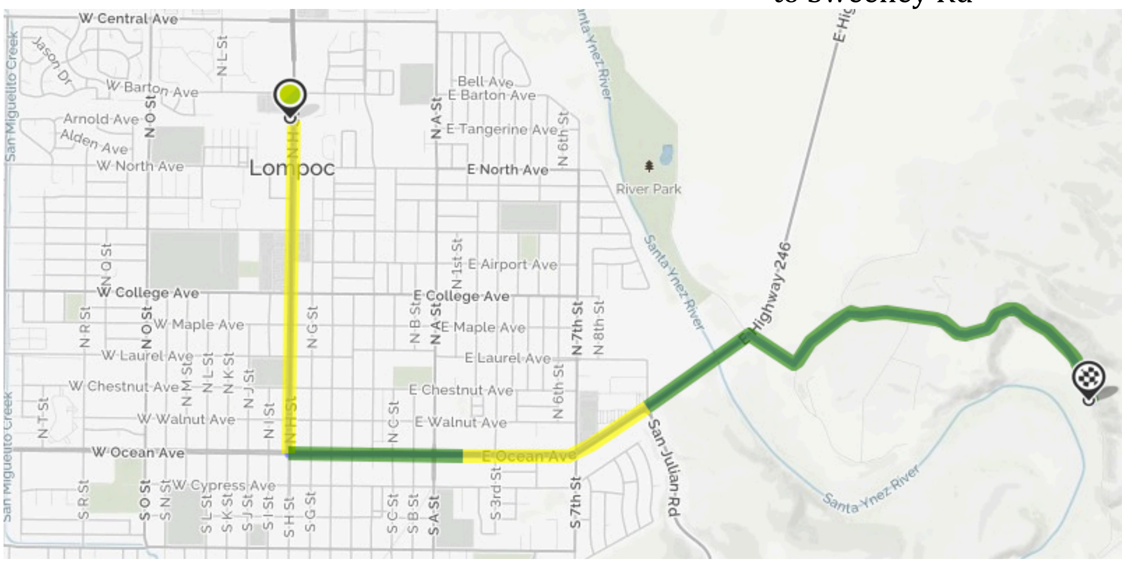

Driving directions to Stop 1: Sweeney Rd., Lompoc, CA

Route	**Distance**
Exit Parking lot and turn right (head south) on N H St/CA-1	1.2 mi
Turn left onto E Ocean Ave/CA-246. Continue to follow CA-246	1.7 mi
Turn right onto Sweeney Rd and drive to outcrop on left	1.5 mi

Stop 2: Vandenberg Air Force Base, Lompoc, CA
-120.5206° 34.7509°
Mapquest map from Sweeney Rd to air force base front gates.
Check in at Visitor's Center. Restroom stop.

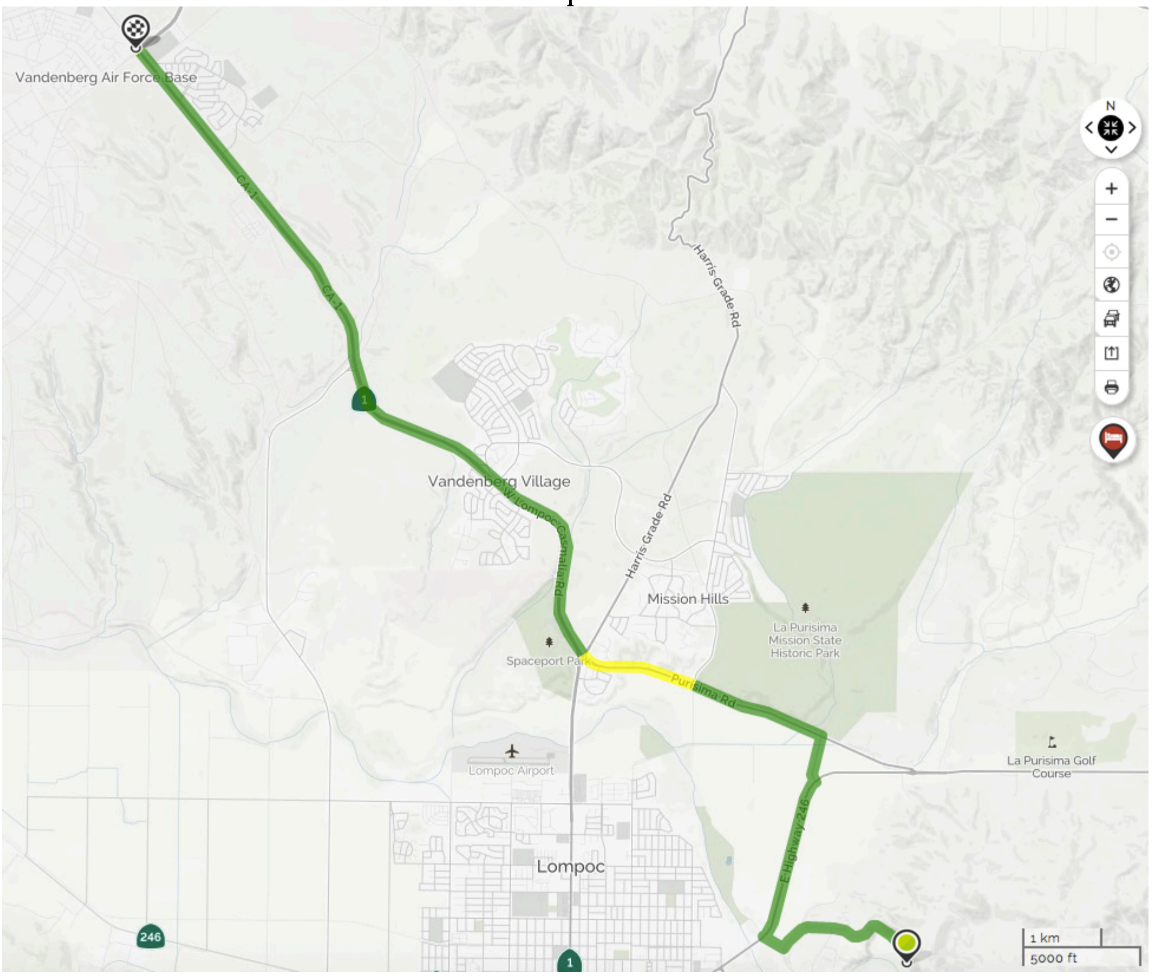

Driving directions to Stop 2: Vandenberg Air Force Base, Lompoc, CA

Route	Distance
Drive west on Sweeney Rd to return to CA-246	1.5 mi
Turn right onto E Highway 246/CA-246	1.4 mi
Turn left onto Mission Gate Rd	0.4 mi
Take the 1st left onto Purisima Rd	2.1 mi
Purisima Rd becomes CA-1/W Lompoc Casmalia Rd (stay R for northbound	6.6 mi
Turn right on CA-1 and make first U-turn (left) to enter the base. Turn right immediately to Visitor's Center (first parking lot on the right)	0.2 mi

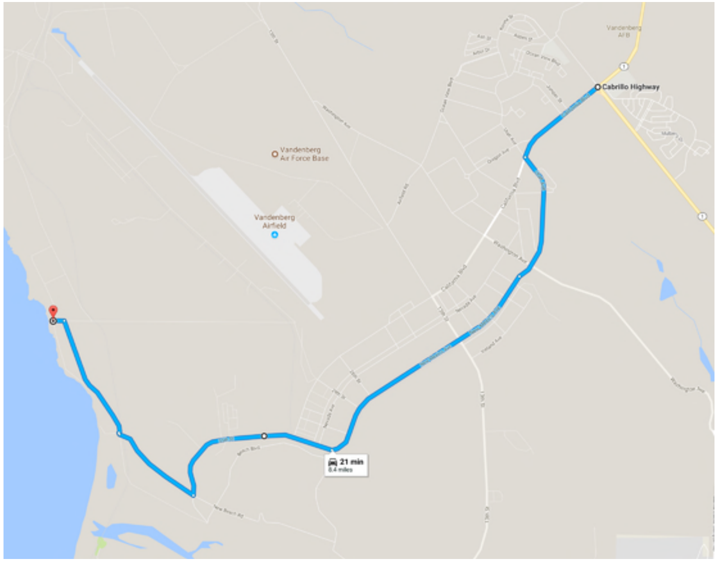

Stop 3: Lompoc Landing, Vandenberg Air Force Base, Lompoc, CA
-120.6084° 34.7202°
Mapquest map from Visitor's Center to Lompoc Landing. ~30 minutes. Be aware of rocky terrain and waves.

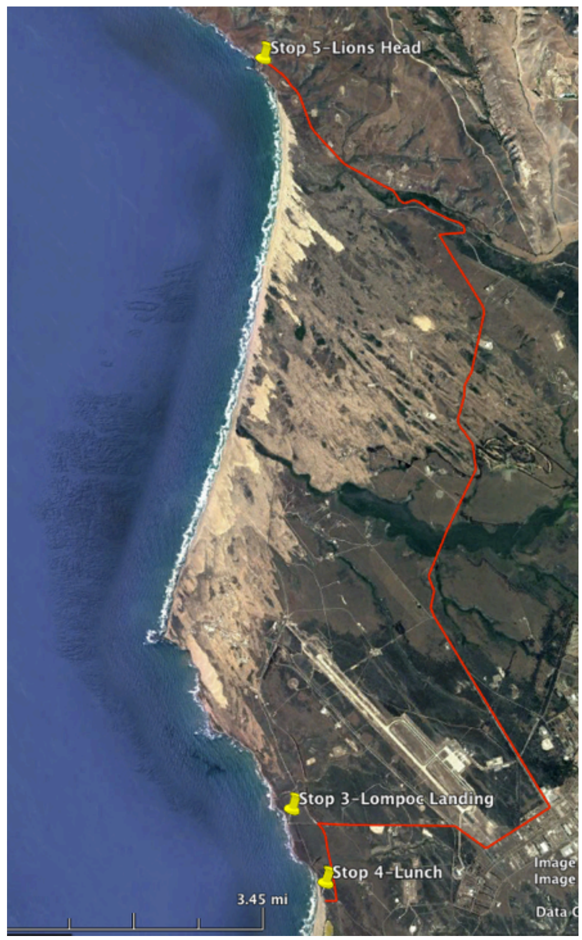

Stop 4: Lunch stop, Vandenberg Air Force Base, Lompoc, CA
-120.6005° 34.7061°
Google Earth map from Lompoc Landing to beach. ~15 minutes.

Stop 5: Lions Head, Vandenberg Air Force Base, Lompoc, CA
-120.6155° 34.8649°
Google Earth map from beach to Lions Head. ~45 minutes.

Stop 0: Embassy Suites by Hilton Central Coast parking lot, Lompoc, CA
-120.4587° 34.6559°
Mapquest map from Lions Head to hotel. ~45 minutes (23 mi).

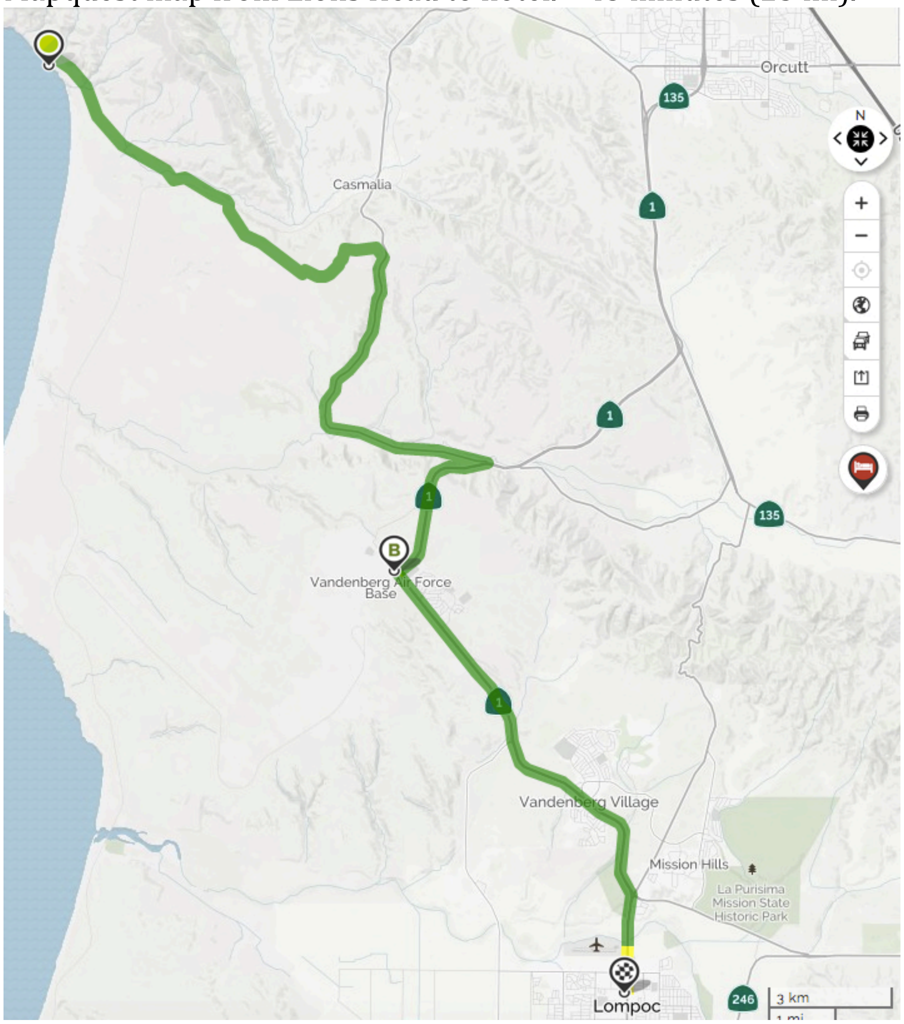

Monterey(!) Petroleum System of the Onshore Santa Maria Basin

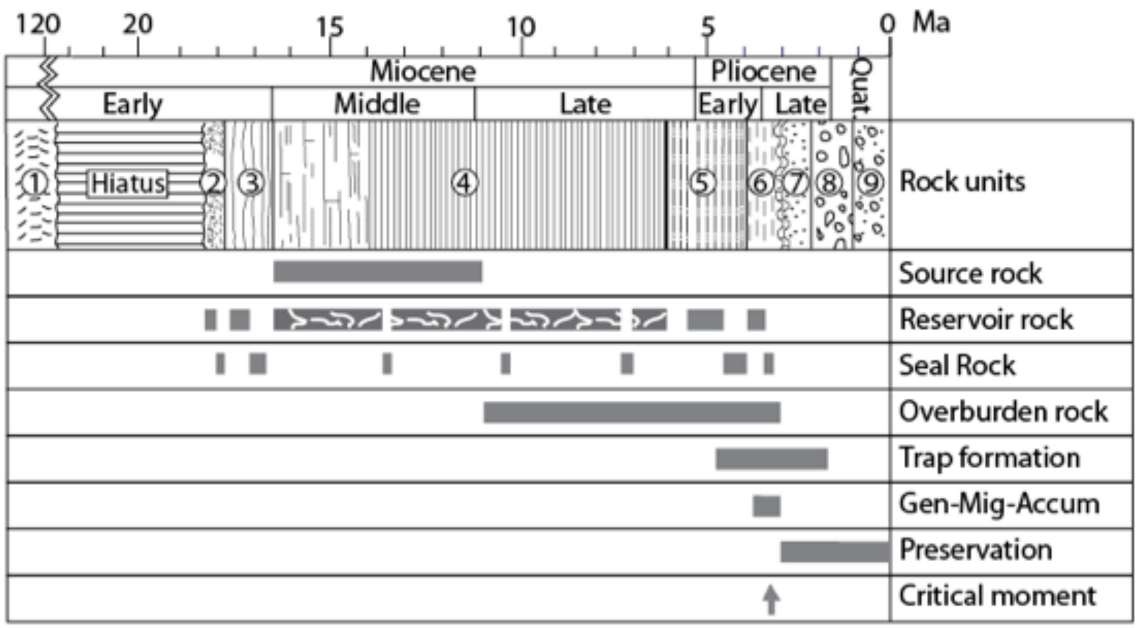

1 Franciscan Complex; 2 Lospe Fm. (alluvial fans, lakes); 3 Point Sal Fm. (submarine fan); 4 Monterey Fm. (hemipelagic: upper middle bathyal 500-1500m); 5 Sisquoc Fm. (upper bathyal 150-500m); 6 Foxen Mudstone (upper bathyal); 7 Careaga Sandstone (nearshore marine); 8 Paso Robles Fm. (streams, lakes); 9 Alluvium, dune sands (streams, beaches).

Figure 1. Events chart for the Monterey (!) petroleum system.

Summary of Petroleum System Elements
Source Rock: middle Miocene lower Monterey Formation
Reservoir Rock: fractured Monterey Formation
Seal Rock: Opal-A and opal-CT phase Sisquoc and mudstones throughout the section
Overburden Rock: late Miocene Monterey Formation, Sisquoc Formation, Foxen Mudstone
Trap Timing: beginning 6 Ma when Pacific-North American transform margin became compressive; continuing in Pliocene to Quaternary with intense shortening
Generation-Migration-Accumulation: Generation began about 5 Ma
Critical Moment: 4 Ma

Summary: Sweeney Road

Location: Southern edge of Santa Maria Basin
Petroleum system element: Overburden rock
Geologic units:

- Sisquoc Formation (5 to 6 Ma)
- Monterey Formation (6 to 8 Ma) clayey-siliceous member (uppermost)

Silica phase:

- Opal-A in Sisquoc Formation
- Opal- A and Opal-CT in Monterey Formation

Lithologic features:

- Interbedded laminated and massive intervals of diatomite and diatomaceous mudstone in Sisquoc
- Ribbon-bedded opal-CT chert and porcelanite in Monterey

Structural features:

- Kilometer-scale anticlines and synclines (part of E-W striking fold belt)
- Centimeter to meter scale folds
- Contrast in bed-to-bed mechanical features

Summary: Lompoc Landing

Location: Western edge of Santa Maria Basin at coast
Petroleum system element: Reservoir rock
Geologic units:

- Monterey Formation (11 Ma) upper calcareous siliceous member

Silica phase:

- Opal-CT in initial stages of conversion to quartz

Lithologic features:

- Opal-CT and quartz chert breccia
- Exhumed oil accumulation within fractured chert and porcelanite
- Interbedded siliceous shale

Structural features:

- Near crest of large anticline south of Lompoc-Purisima anticlinal trend
- Bed confined fractures, through-going fractures, asphalt-filled fractures, and asphalt breccia zones/dikes

Summary: Lions Head

Location: Northwestern edge of Santa Maria Basin at coast
Petroleum system element: Source rock, Reservoir rock
Geologic units:

- Monterey Formation (11 to 16 Ma) lower calcareous-siliceous member, phosphatic member, upper calcareous siliceous member

Silica phase:

- Quartz

Lithologic features:

- Point Sal Ophiolite in fault contact with lower Monterey Formation
- Laterally persistent dolostone bed, phosphatic lenses, tiger-stripe chert

Structural features:

- Contorted and buckled quartz-phase chert, faulting and fracturing

Introduction

For this, the 10th Annual Stanford Basin and Petroleum System Modeling Industrial Affiliates Meeting, we visit the onshore Santa Maria Basin, a roughly triangular shaped sedimentary basin located north of the Santa Barbara-Ventura Basin and south of the Pismo Basin (**Figure 2**). The Santa Maria Basin is bound on all sides by fault zones: the Santa Ynez River fault forms the southern border, the Santa Maria River fault comprises the northern margin, and the Hosgri fault offshore marks the western boundary (**Figure 3**). Wedged between the Coast and Transverse Ranges (**Figure 4**), the geologic configuration of petroleum system units in the Santa Maria Basin is thus closely tied to the tectonic history over the past ~20 m.y.

Although native peoples from the Chumash tribe likely used asphalt from surface seeps for sealing their canoes and baskets (MacKinnon, 1989), the Santa Maria Basin was discovered to be an economic petroliferous province in 1901 when the Western Union Oil Company produced paying quantities of oil in their third prospect hole in what is now the Orcutt field (Arnold and Anderson, 1907). As of 2009, about 880 MMBO of oil and 850 MMCF of associated gas have been produced from this basin (CA DOGGR, 2010).

The outcrops visited on this trip take us top-down through the petroleum system—as if drilling a well:

- the overburden rock, late Miocene upper Monterey and late Miocene-to-early Pliocene Sisquoc formations at Sweeney Road
- the principal reservoir rock, late Miocene upper Monterey Formation at Lompoc Landing, Vandenberg Air Force Base; and
- the petroleum source rock, middle Miocene lower Monterey Formation at Lions Head, Vandenberg Air Force Base

Along the way, we will discuss regional tectonics, silica diagenesis, paleo depositional environments, tectonic deformation and petroleum system development.

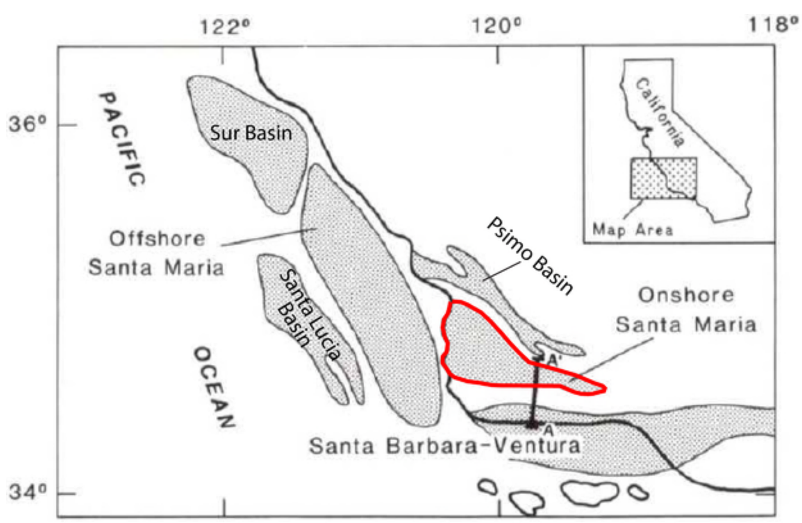

Figure 2. Location of onshore Santa Maria Basin (red outline) relative to other nearby, primarily Miocene age basins in central California. Modified from Keller (1990).

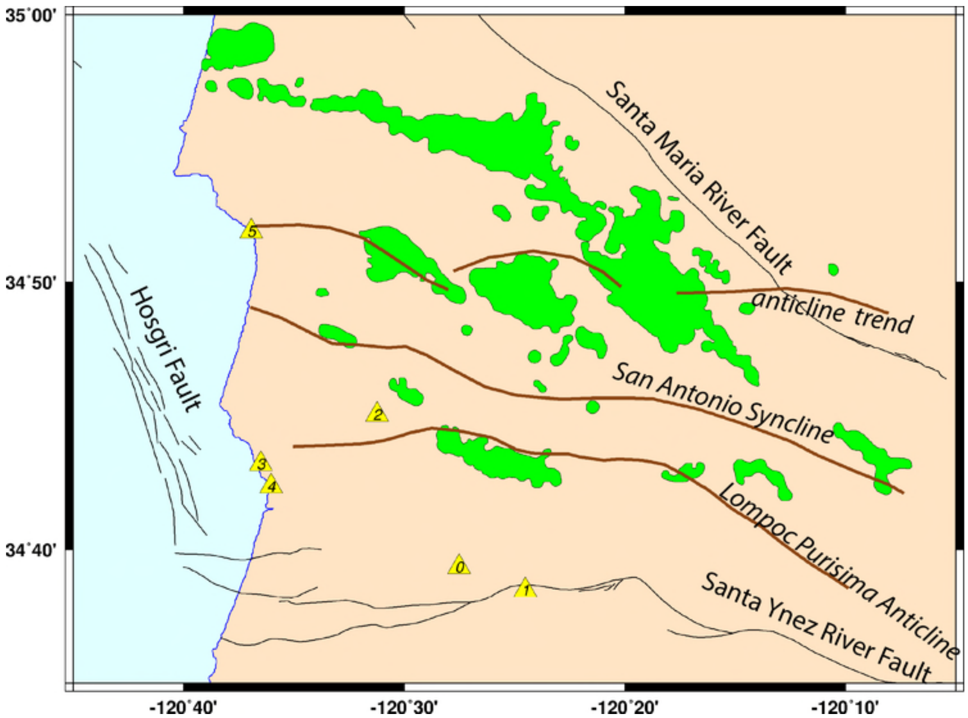

Figure 3. Onshore Santa Maria Basin with oil fields (green-filled polygons. Field trip stops (triangles): 0, Embassy Suites, Lompoc; 1, Sweeney Road; 2, Vandenberg Air Force Base 3, Lompoc Landing; 4, lunch; 5, Lions Head. Labeled faults from USGS (2017). Structural lineations (brown lines) from Namson and Davis (1990).

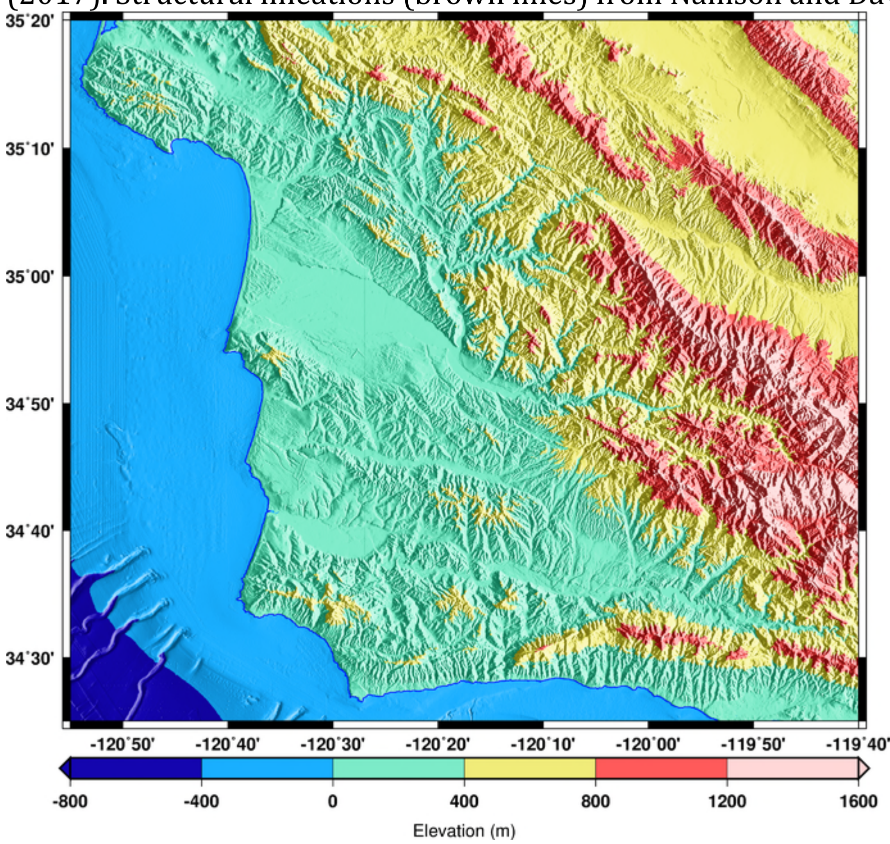

Figure 4. Topography map of the Santa Maria Basin. Digital elevation model is a 30 arc-sec (90m) resolution grid from NOAA (2017).

Regional Geology and Tectonics

Although the Santa Maria Basin is inherently a Miocene basin, with sedimentary fill dating from about 18 Ma to present, its ancient history as part of California's subduction margin is evident in the metamorphic and volcanic rocks of the Point Sal Ophiolite, which we will see at the final field trip stop in fault contact with the Monterey Formation. The tectonic history of the onshore Santa Maria Basin is complex and a full treatment is beyond the scope of this field trip guide. Generally, though, the Miocene history of the basin can be summarized with four main phases: rifting with attendant subsidence in the early Miocene; middle to late Miocene deposition and compaction; early Pliocene contraction; and late Pliocene to Holocene contraction (Gutiérrez-Alonso and Gross, 1997).

The early Miocene extensional stage is tied to cessation of subduction and transition to transform margin tectonics that spawned several borderland marine basins in California (MacKinnon, 1989; McCrory et al., 1995). Timing of this transition is pinned at about 17.5 Ma by radiometric age dating of basal volcanics in the Lospe Formation (Stanley et al., 1995). Both the Lospe and overlying Point Sal formations, which underlie the Monterey Formation in the Santa Maria Basin, contain negligble but non-zero quantities of oil (**Figure 5**). More importantly, the two formations record the earliest phase of basin subsidence: paleowater depths increased dramatically from near-zero for the basal nonmarine to marine conglomerate of the Lospe Formation to about 3300 ft (1000 m) with deposition of the deep-water sands and interbedded mudstone of the Point Sal Formation (Dunham and Cotton-Thorton, 1990; McCrory et al., 1995).

Subsidence occurred rapidly at first, from about 18 to 16 Ma, associated with block rotation of the western Transverse Ranges then slowed during the thermal subsidence phase from about 16 to 7 Ma (McCrory et al., 1995). This pattern of very rapid subsidence followed by an extended period of slow subsidence is typical of basins associated with slab windows in California (Wilson et al., 2005). During this period of tectonic quiescence, the principal rock of interest on this field trip was deposited: the Monterey Formation. Beginning about 16 Ma, terrigenous-derived clastic sedimentation ceased, marking the beginning of a ~10 m.y. long period of fine-grained deposition—clay, silt, and calcareous and siliceous ooze.

California's "superstar" oil producer, the Monterey Formation, is the subject of countless studies and is particularly well analyzed along the central California coast. Landmark studies by Carolyn Isaacs and co-authors (Isaacs, 1981a, b, c, 1992, 2001; Isaacs and Rullkötter, 2001) established the fundamental stratigaphy of the Monterey Formation and tied it observed variations to changing ocean conditions. The stratigraphy and even the age boundaries of the Monterey formation vary among California marine basins but generally consists in the Santa Maria Basin of, from base to top, a calcareous-siliceous member, a middle phosphatic member, a middle carbonaceous marl, and a clayey-siliceous upper member (**Figure 6**) (MacKinnon, 1989). The thickness of the Monterey Formation in the Santa Maria Basin is about 3370 ft (1150 m)—or about 3 times that in the extensively studied east-west section of the Santa Barbara coast.

The key lithologic aspect of the Monterey Formation is its biosiliceous character. Biosiliceous sediments are prevalent around the northern Pacific rim, in offshore Japan and California, and in the Norwegian Sea (Ingle, 1981). These biogeneous sediments have their origins in high productivity, coastal upwelling conditions in which microorganisms—radiolarian and diatoms— rain to the seafloor and become a silica-rich "ooze." When deposited, that silica is in its opal-A phase, which has an amorphous crystal habit and is thermodynamically unstable at temperatures above about 40°C and burial depths of about 1650 ft (500 m) (**Figure 7**). With increasing burial (and thus, heating), silica transforms from its disordered opal-A phase to a thermodynamically more stable one, opal-CT. Even more burial results in the most stable silica form of all, quartz (**Figure 7**).

It is important to emphasize that the diagenetic phases of silica transformation are often used interchangeably with rock types. That is, a rock with silica chiefly in the opal-A form is often thought of as diatomite, a rock with mostly opal-CT as porcelanite, and a rock with mainly quartz as chert. The bottom panel of **Figure 7** emphasizes the need to distinguish the lithologic character of a rock (i.e., what it is called) from the diagenetic grade of silica. A rock with silica predominantly in the opal-CT phase can thus be called shale, siliceous shale, porcelanite, or chert, for example, depending on the relative weight of biogenic silica (**Figure 7**). This is important to remember at Lions Head, where quartz-phase rocks are present in shales, siliceous shales, porcelanites, and cherts.

Although the depth of burial is the chief control on silica crystal habit, a critical factor is the relative percentage of detrital clay (Keller and Isaacs, 1985) (**Figure 7**). A variety of other factors affect the kinetics of silica diagenesis (Behl and Garrison, 1994), such as organic carbon (Dralus, 2013), but that is beyond the scope of this guide. What makes the transformation of silica so significant for petroleum provinces is the change in mineral density that accompanies each phase change—from 1.8 g/cc for opal-A to 2.3 g/cc for cristobalite and tridymite forming opal-CT), and to 2.65 g/cc for quartz. A significant volume of silica is added at each phase change in the form of pore-filling cement (Behl and Garrison, 1994). Thus, with compaction, these step-wise increases in density produce step-wise decreases in porosity (**Figure 7**). Matrix permeability similarly drops, but because increasing amounts of opal-CT and quartz increase rock brittleness, fracture permeability tends to increase due to natural fracturing.

A change in the relative angle of motion between the Pacific and North American plates at 6 Ma put the plate boundary into transpression and thus initiated a period of uplift and crustal shortening in the Santa Maria Basin (McCrory et al., 1995). Biogenic silica deposition continued, but the consequent increase in terrigenous influx into the Santa Maria Basin marked the end of Monterey deposition and the beginning of Sisquoc deposition (**Figure 5**). Silica in the opal-A phase through most of the Sisquoc indicates it was never deeply buried. The contact between the Monterey and the Sisquoc formations can be conformable, such as at Sweeney Road (field trip stop 1), both outcrops and subsurface wells record erosional unconformities between the units, likely a result of tectonic activity on basin margins (Behl, 2000; Ramirez and Garrison, 1995).

Overlying the Sisquoc Formation both conformably and unconformably is the Foxen Mudstone, a siltstone and fine-grained sandstone, which itself is overlain by the upper Pliocene Careaga Sandstone. Together these units record the shoaling of the Santa Maria Basin and the end of marine conditions (McCrory et al., 1995). The Careaga Sandstone and younger units play no role in petroleum system development in the Santa Maria because they post-date the generation-migration-accumulation of petroleum (**Figure 5**).

A second episode of orogeny began in the Late Pliocene or Quaternary and continues today, building the modern Santa Maria Fold and Thrust Belt (Namson and Davis, 1990). This more intense contractional phase relative to the earlier phase intensified structural closure in existing traps (Namson and Davis, 1990).

As a final thought, it is worth pointing out that the onshore Santa Maria Basin is a distinct petroleum province from the one offshore. The offshore Santa Maria Basin is located on the west side of the Hosgri Fault, a feature that was a major strand of the San Andreas Fault in the late Miocene (Dickinson et al., 2005) when the onshore Monterey(!) petroleum system was actively generating petroleum. Thus, the two basins were not contiguous during key processes in petroleum system development onshore.

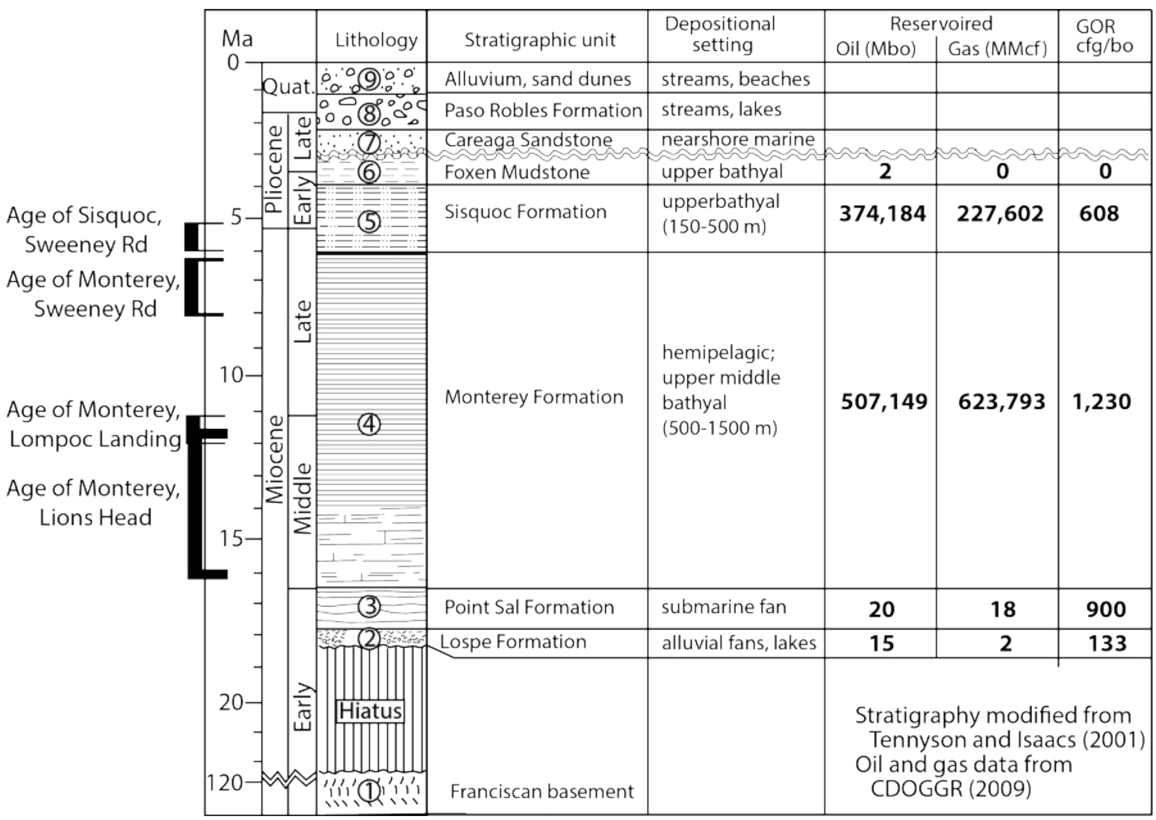

Figure 5. Stratigraphy of the onshore Santa Maria Basin modified from Tennyson and Isaacs (2001). Oil and gas statistics are from California Division of Oil, Gas, and Geothermal Resources (CDOGGR, 2010). The numbers on the rock units refer to numbered units on the Events Chart (**Figure 1**).

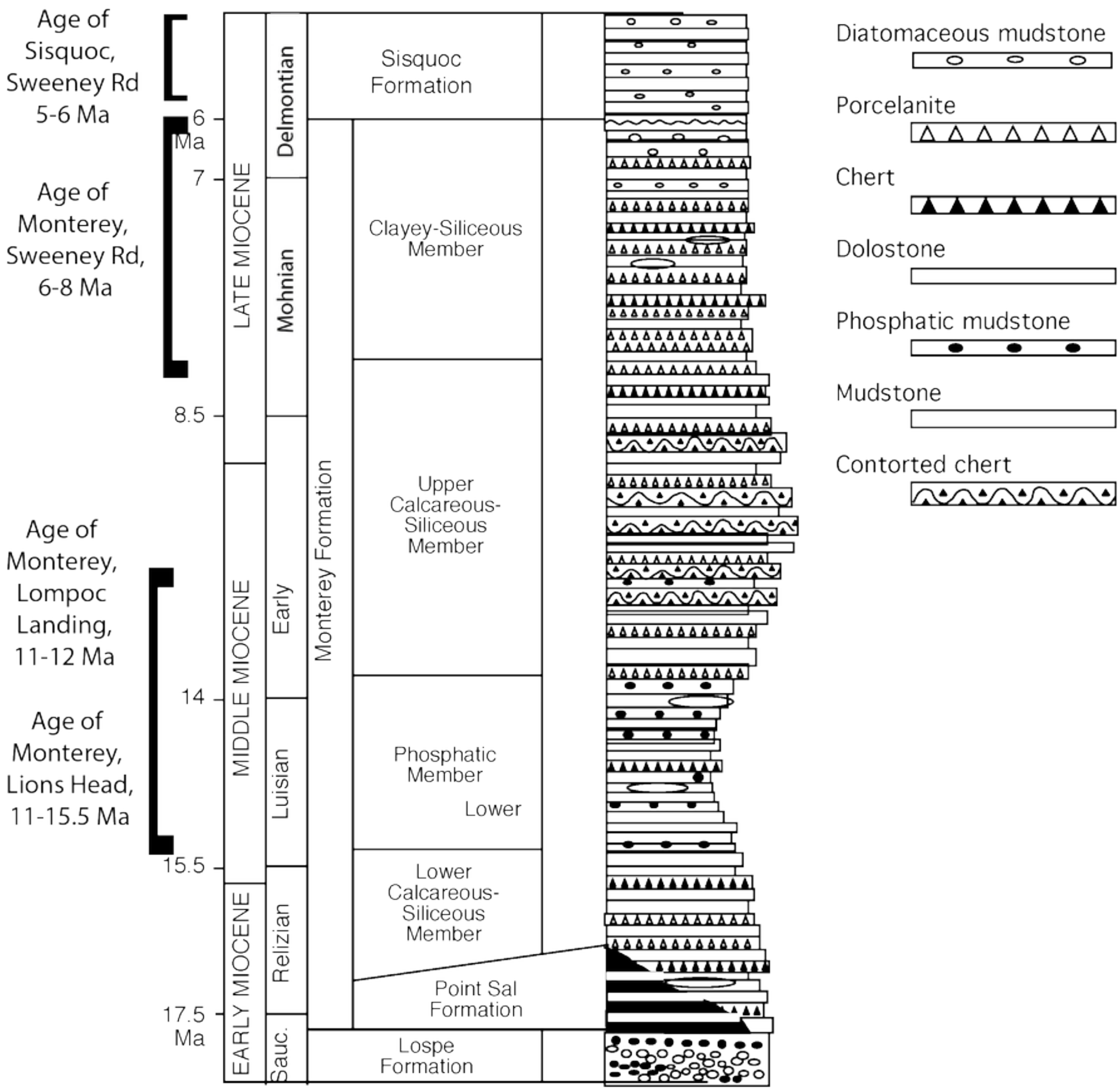

Figure 6. Stratigraphic members of the Monterey Formation in the Santa Maria Basin. Figure is based on MacKinnon (1989) and modified by Rick Behl.

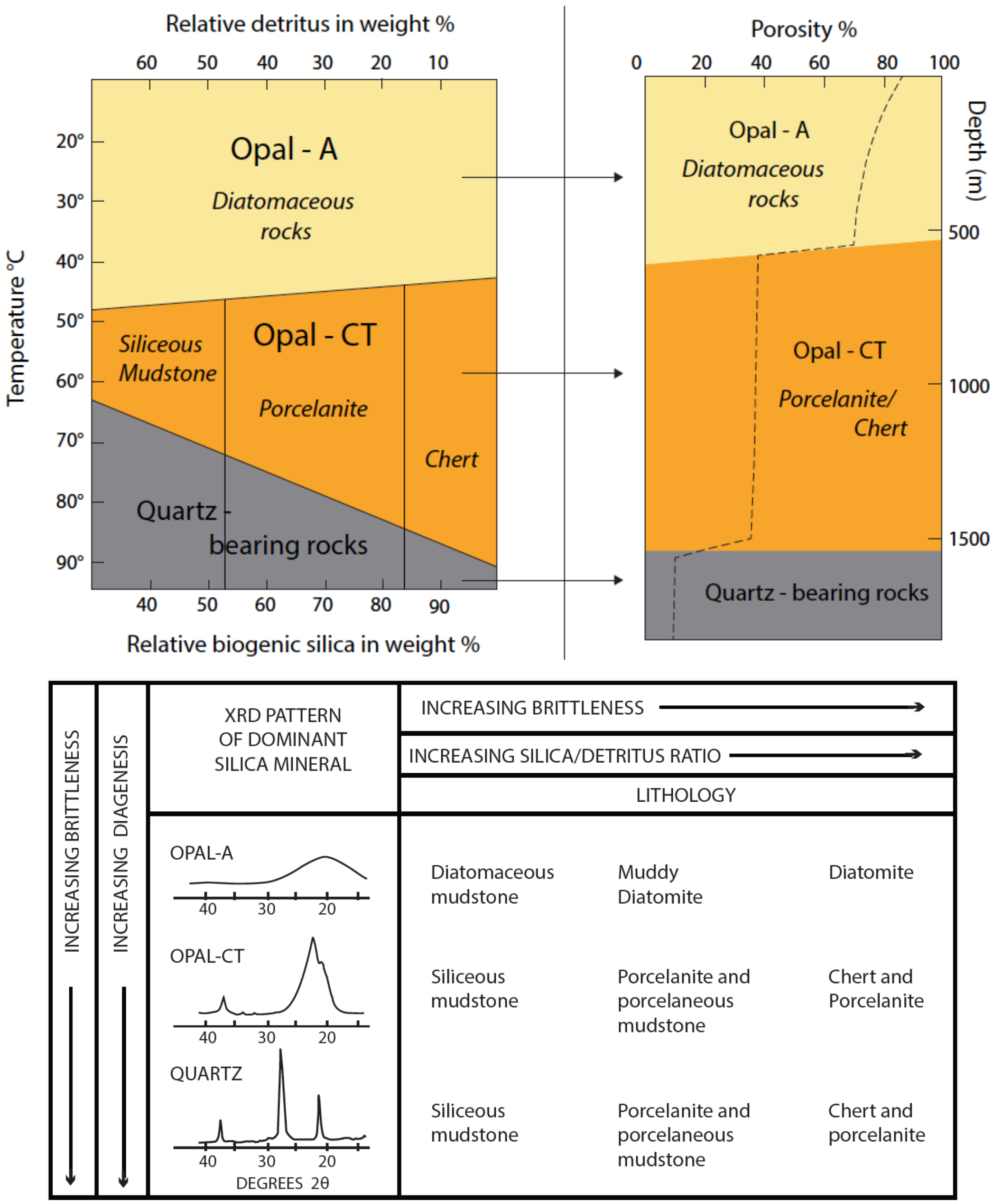

Figure 7. Top two panels are from Wirtz (2017) as modified from seminal work by Issacs (1981c) among others. Bottom panel is from Snyder et al. (1983) and Pisciotto and Garrison (1981) as modified by Ryan Weller.

Essential elements of the petroleum system

Source Rock

Geochemical correlation of biological markers by Curiale et al. (1985) established the genetic link between oil samples and Monterey source rock in the Santa Maria Basin. Michael (2001) performed a similar oil-rock correlation study and confirmed with biomarkers a source signature of calcareous-siliciclastic, corresponding to the lower member of the Monterey Formation. Careful accounting of all pools in the basin shows that the major reservoir rock is also the Monterey Formation, responsible for ~600 MMBOE (**Table 1**). Thus, following the naming convention for petroleum systems established by Magoon and Dow (1994), the name and level of certainty of this petroleum system is Monterey(!).

The most comprehensive treatment that we know of concerning the organic properties of the basal Monterey source rock is from the outcrop at Lions Head on Vandenberg Air Force Base (stop 5 on this field trip). These properties are detailed and compared/contrasted with the source rock at Naples Beach in the Santa Barbara-Ventura Basin in a seminal volume by Isaacs and Rutköller (2001).

The basal lithology of the Monterey at Lions Head is clay mudstone and dolomite, mostly in the phosphatic member (**Figure 6**); this correlates with the organic shale member (later renamed the carbonaceous marl member) described by Isaacs (1981a) in coastal outcrops near Santa Barbara. Total organic carbon (TOC), a measure of source rock quantity, of the lower member exceeds 2 weight percent, which qualifies as "Very Good" to "Excellent" in the evaluation scheme of Peters and Cassa (1994). Several more samples within this same section corroborate this finding (Katz and Royle, 2001).

Hydrogen index (HI) ranges from about 475 to about 600 (Katz and Royle, 2001), indicating type I oil-prone source rock (**Figure 8**). The production index (PI <0.10), T_{max} (T<435°C) and vitrinite reflectance (<0.6 %Ro) all indicate that the Monterey source rock at Lions Head is thermally immature. Thus, these TOC and HI values are "original" and so are representative of the petroleum generative capacity of the source rock (e.g., Peters et al., 2005).

There is significant discussion in the literature about the Monterey Formation in the Santa Maria Basin containing high-sulfur kerogen and that this causes the source rock to thermally mature earlier (at lower temperatures) than low-sulfur kerogen (Orr, 2001). Our initial investigation into the Monterey(!) petroleum system is beginning to call this into question for at least the basal part of the Monterey Formation in the Santa Maria Basin. For example, the lowermost samples in the Lions Head section contain less sulfur than samples higher in the section, confirming that the basal Monterey source rock as typified by the Lions Head outcrop is not high in sulfur (Michael, 2001). Furthermore, HI values exceed 300 mg HC/g TOC for all measured samples, indicating that at least at Lions Head, the Monterey is very near the type I-type II kerogen boundary rather than the typically assumed type II-S. Perhaps more definitively, kinetic profiles of the kerogen from immature Monterey source rock at Lions Head overlay the kinetics for type II Kimmeridge Shale, which is not sulfur rich. Both of those curves differ significantly from those for the sulfur-rich kerogen at Naples Beach in the Santa Barbara-Ventura Basin to the south (Jarvie and Lundell, 2001). In that more southerly basin, oxygen appears to play an important role in the fast reaction of the high-sulfur kerogen; there is very little oxygen in the kerogen at Lions Head (Jarvie and Lundell, 2001).

Finally, a recent comprehensive geochemistry study of oil samples from the Santa Maria Basin may eventually lead to refinement of the particular facies in the Miocene Monterey source rock that have generated oil Peters et al. (this volume). Three main oil families are defined on the basis of hierarchical cluster analysis of 21 biomarker and isotope ratios (**Figure 9**). Family 2 is based on just a few samples and is geographically restricted to the far southeast side of the basin (blue triangles, **Figure 9**) whereas the other two families show systematic distributions in the three tectonic corridors previously defined by Namson and Davis (1990).

Clearly several lines of inquiry remain as to the nature of the Monterey source rock in the onshore Santa Maria Basin.

Voilume of Oil and Gas by Reservoir Rock in the Monterey(!)

Reservoir Rock	Pools	Yr Dis	Oil (Mbbl)	%	Gas (MMcf)	%	BOE (Mbbl)	%	GOR (ft3/bbl)	API	Sulfur (wt %)
Foxen	3	1965-1977	2	0.0	0	0.0	2	0.0	10	12.0	nd
Sisquoc	8	1941-1979	374,184	42.5	227,602	26.7	412,118	40.3	608	15.0	5.0
Monterey	31	1903-1885	507,149	57.5	623,793	73.3	611,115	59.7	1,230	7 to 36	0.2 to 8.0
Pt Sal	2	1983-1985	20	0.0	18	0.0	13	0.0	900	30.0	0.61
Lospe	1	1985	15	0.0	2	0.0	15	0.0	133	33.0	1.65
		TOTAL:	881,370		851,415		1,023,263	100.0			

Table 1. Table of petroleum accumulations organized by reservoir rock in the Santa Maria Basin.

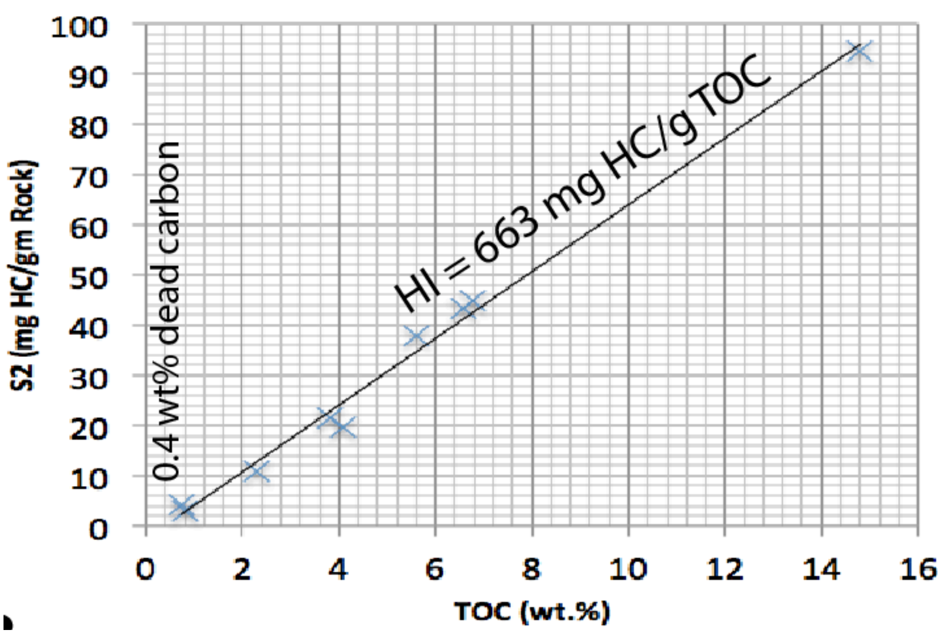

Figure 8. The S2 vs TOC plot indicates an HI for the basal Monterey source rock of 660 mg HC/g TOC. This source interval has 0.4 wt % inert or dead carbon.

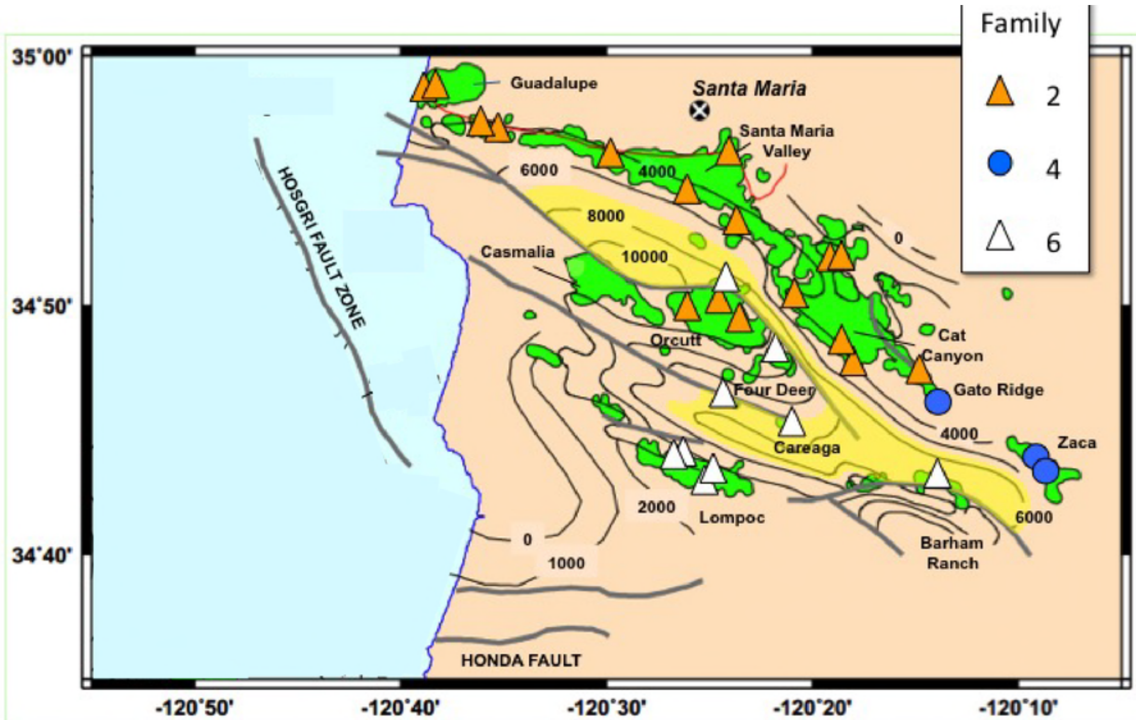

Figure 9. Oil families defined by Peters et al. (this volume) for the onshore Santa Maria Basin. Pod of active source rock (yellow shading) mapped by Tennyson and Isaacs (2001).

Reservoir Rock

The success of the Monterey Formation as a reservoir rock in the Santa Maria Basin is due to the embrittlement associated with the diagenetic transformation of diatomaceous rocks to porcelanite and chert. Without this chemical alteration of silica, the Santa Maria Basin would likely lack suitable reservoir rock facies altogether due to its relative isolation from the North American mainland, which hampered development of turbidite sandstone reservoirs that produce so prolifically in the nearby San Joaquin and Los Angeles basins. Fractured dolomite and dolomitic mudstone are very important reservoir rocks in many fields and stratigraphic intervals as well.

Can we thus define the Monterey(!) as an "unconventional" petroleum system in the Santa Maria Basin as a consequence of oil generation, migration, and accumulation within the fine-grained rock itself? The answer is "no" if an unconventional petroleum systems is defined as requiring artificial stimulation (e.g., Holditch, 2006). Rather, the Monterey Formation can be considered to be "naturally stimulated" as a consequence of silica diagenesis: although both *matrix* porosity and permeability generally decrease with each stage of silica transformation, *fracture* porosity and permeability both increase, although the effect is much more significant for fracture permeability (MacKinnon, 1989). In the Monterey Formation, brecciated chert reservoir rocks have the smallest fracture spacing and largest fracture permeability, followed closely by chert and porcelanite (Namson and Davis, 1990). These fractures link (described below for Lompoc Landing) throughout the formation to form natural migration pathways.

The Sisquoc Formation is the second largest reservoir rock in the onshore Santa Maria Basin, having produced ~600 MMBOE. This is likely is a consequence of sitting immediately above the heavily fractured, oil-soaked Monterey, which likely leaks into the Sisquoc above. In places, the Sisquoc Formation has a basal sand member consisting of eroded Monterey and Point Sal grains; this can be charged with oil and sealed by overlying diatameceous mudstone (Dunham and Cotton-Thorton, 1990). Oil may also migrate vertically from the Monterey to the Sisquoc via pebbly dikes, or injectites, as evidenced by several cores from the Casmalia Hills in the northwestern part of the basin (Henderson, 1990).

Seal Rock

The Monterey(!) petroleum system is sealed by low-permeability lithologies overlying the source rock. The Sisquoc Formation acts as both a reservoir rock and seal rock in the basin: because it is biosiliceous and brittle, petroleum from the Monterey Formation naturally leaks into the Sisquoc above, but where rich in clay, the Sisquoc is sealing. The overlying Foxen Mudstone, however, contains almost no oil (**Figure 5**) and is thus an excellent seal rock.

Overburden Rock

Accumulation rates for the Monterey Formation appear low at Lions Head, where stratigraphic thickness and age indicate that the basal member accumulated at 54 m/m.y. and the exposed part of the middle member accumulated at 32 m/m.y. (**Figure 10**). However, linear sedimentation rates are not really applicable to these quartz-phase rocks. Nevertheless, by the end of Monterey deposition, the basal source interval in this outcrop was insufficiently buried to be thermally mature for petroleum generation. As in other sedimentary basins in California, thermal maturation of the Monterey source rock only became possible in Pliocene times, when bordering highlands began to shed large quantities of clastics into nearby marine basins. With deposition of the Sisquoc Formation in the Santa Maria Basin, accumulation rates jumped by an order of magnitude relative to the Monterey Formation: the basal 650 ft (200 m) of the Sisquoc at Sweeney Road accumulated at 600 m/m.y. and the exposed part of the overlying 200 m accumulated at 280 m/my; these numbers are uncorrected for the effects of compaction (Dumont and Barron, 1995) (**Figure 10**). These extreme sedimentation rates show that a source rock deposited millions of years before can be thermally matured in just a few million years time.

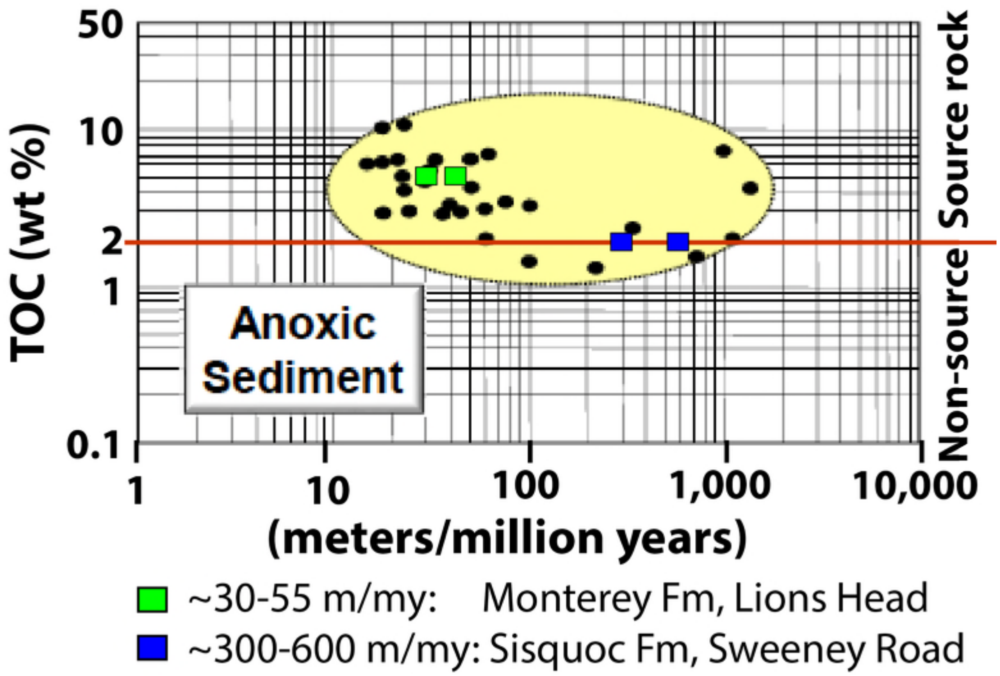

Figure 10. Sedimentation rate for the Monterey and Sisquoc formations at outcrop locations in the Santa Maria Basin. TOC, Total Organic Carbon. Average TOC for the Monterey Formation is from outcrop samples at Lions Head analyzed by Katz and Royle (2001); sedimentation rate is calculated by us using stratigraphic thickness and ages in Isaacs and Rutköller (2001). Average TOC for the Sisquoc Formation is from subsurface wells analyzed by Isaacs and Tomson (1990); sedimentation rate is from Dumont and Barron (1995). Filled circles are data from Pelet (1987). Red horizontal line separates source rocks, defined as TOC>=2 wt %, from non-source rocks.

Generation

Early work suggested that the large volume of low gravity, high sulfur oil in the basin was generated from the Monterey Formation at low thermal maturity, low temperatures, and shallow depths (Orr, 2001). Our research on this petroleum system is beginning to call into question this "sacred cow," as discussed above. The pod of active source rock as mapped by Tennyson and Isaacs (2001) (see **Figure 9)** is drawn on the basis of a fast-reacting, high-sulfur kerogen; moreover, its shape appears to be controlled by structures that are much younger than the petroleum system. We suggest that a more robust way to map the pod of active source rock is to restore the depth to the oil window to its paleo depth. Thermal maturity indicators such as atomic H/C and O/C ratios from several wells in the basin reveal that the present-day depth of the early oil window is ~9000 feet (2750 m) (Isaacs and Tomson, 1990). The two main pulses of uplift discussed above likely totaled several thousand feet (e.g., McCrory et al., 1995), suggesting that we can restore the beginning of the oil window to a paleo depth more "normal" for oil generation—~13,000 ft (~ 4000 m). That said, the stratigraphic thickness of the Monterey Formation and younger units is highly variable throughout the basin because of its

complicated tectonic history. A simple restoration of the paleo depth to the pod of active source rock will have to take this variability into account.
Our initial work on the timing of oil generation indicates that overburden rock thickness sufficient to thermally mature the basal Monterey Formation were obtained at the end of Sisquoc deposition, or about 4 Ma.

Migration

The pod of active source rock based on a present-day Monterey depth of 9000 ft (2740 m) indicates that migration distances are up to ten miles (**Figure 11; Figure 12**). Migration occurs laterally and up-dip through connected fractures.

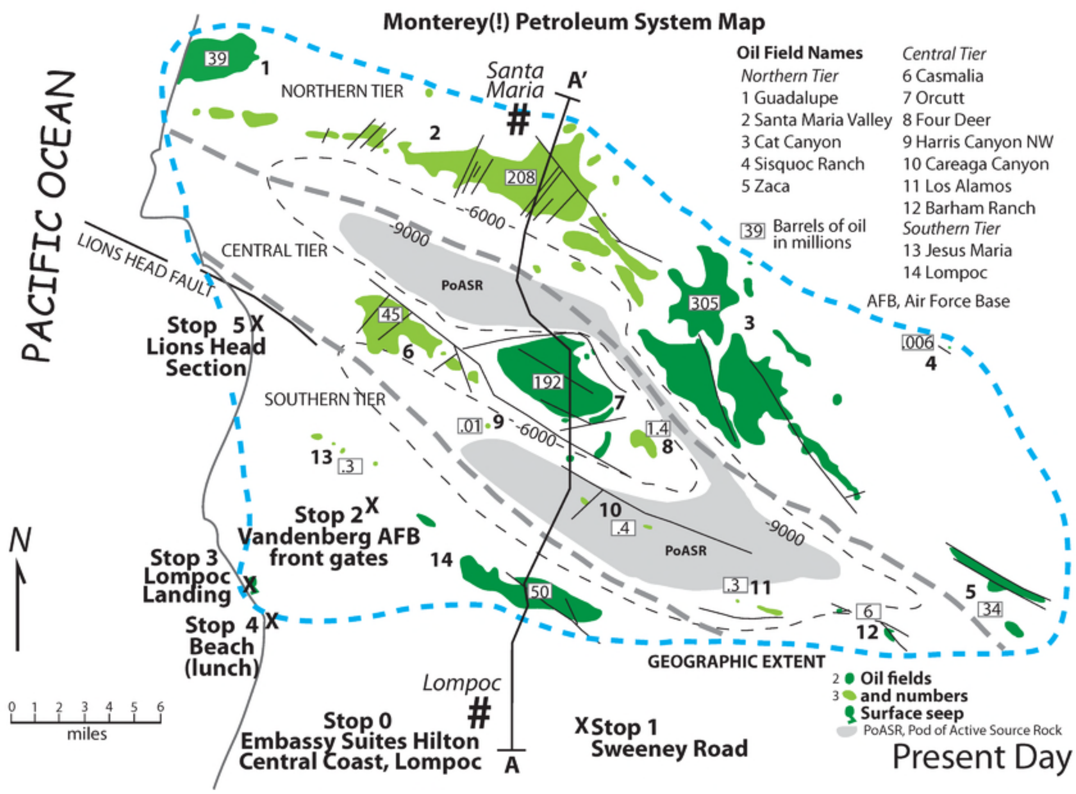

Figure 11. Map of the Monterey(!) petroleum system. Green polygons are known oil fields; same shade of green indicates that nearby pools belong to the same field. Oil fields are divided into a northern, central, and southern tier. Oil in MMBO produced from each field is enclosed by a rectangle. Field trip stops are indicated. Blue dashed line marks the extent of the petroleum system. Depth contours to the top of the Monterey Formation are from Tennyson and Isaacs (2001). Cross-section A-A' is shown in **Figure 12**.

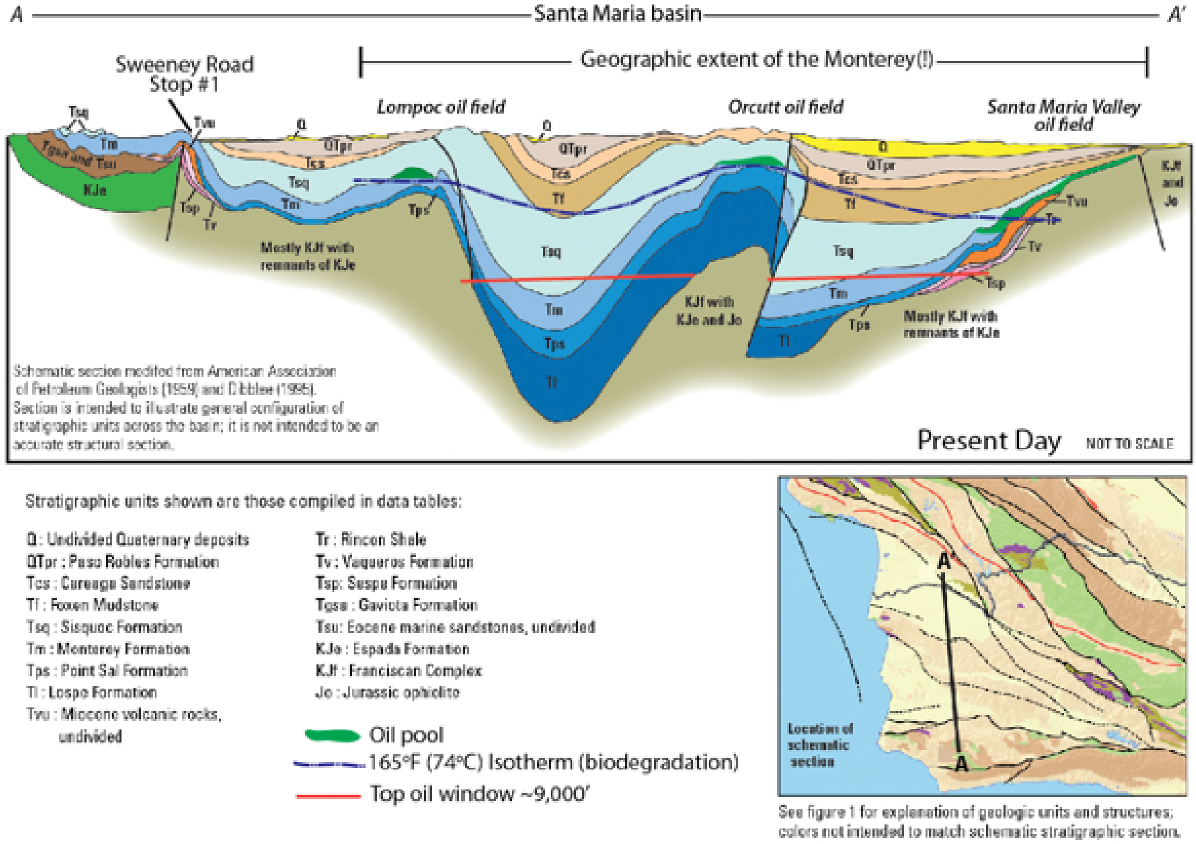

Figure 12. North-south oriented cross-section illustrates sedimentary depocenters, oil pools, depth to the oil window (present-day), and depth of biodegradation. Figure is modified from Sweetkind et al. (2010).

Accumulation

The Santa Maria Basin contains fourteen known oil fields. We divide these fields into geographic groupings on the basis of trapping styles and volumes. The northern tier, in which oil occurs primarily in stratigraphic traps, accounts for 66% of recoverable oil in the basin, most of it in the Santa Maria Valley and Cat Canyon fields (**Figure 11**, **Table 1**). The central tier contains 27 percent of the basin's oil, dominated by the Orcutt field, a structural trap, with the balance (7%) in the southern tier. Interestingly, our groupings of oil fields in the basin compare well with the tectonics–based partitioning of the basin by Namson and Davis (1990), which, from north to south, comprises the Santa Maria Valley, the Casmalia-Orcutt anticlinal trend, and the Lompoc-Purisima anticlinal trend.

A billion barrels of oil equivalent from these 14 fields indicate that the Monterey(!) is a significant petroleum system (**Tables 1, 2**). The three largest fields (>60% of the oil) are structural, stratigraphic, and structural-stratigraphic traps and the other five large fields (~35% of the oil) are structural traps. Generally, the API gravity increases with depth from 5 to 35 API degrees (**Figure 13; Table 2)**. The sulfur decreases with depth from 8 wt. percent to <1 wt. percent. The GOR is less than 2500 cubic feet of gas per barrel of oil, or well within the range of that expelled from a marine source rock. To be sure, there is scatter in each plot.

None of the fields are fully charged. A fully charged oil field, when contoured at the reservoir rock depth, shows the oil-water contact to be at the spill point for the accumulation. The oil accumulations or pools in the fields in this petroleum system show closure deeper than the oil-water contact (**Figure 14**). In other words, the trap could hold more oil than is present today. The unfilled traps could be due to insufficient petroleum charge, structural growth after the trap was filled to the spill point, or both.

The bulk properties of the expelled petroleum in this system can be determined with systematic mapping of data from the fields located within the pod of active source rock. **Figure 15** shows that the region that has generated approximately 15 to 35 API degrees with up to 2 wt. percent sulfur. These bulk properties are similar to expelled oil correlated to the Monterey Formation in the San Joaquin Basin (Lillis and Magoon, 2007). Rather than being generated at low API gravity, a previously proposed, we propose that the API gravity decreased after emplacement due to partial to complete biodegradation of the alkanes.

Monterey(!) Oil Fields, Santa Maria Basin									
Field No.	Name	Mbbl cum	Mbbl ER	Total Mbbl	MMcf cum	MMcf ER	Total MMcf	GOR (ft3/bbl)
1	Guadalupe (abd)	38,546	0	38,546	25,960	0	25,960	673
2	Santa Maria Valley*	206,626	1,033	207,659	260,821	994	261,815	1,261
3	Cat Canyon	303,414	1,719	305,133	183,206	0	183,206	600
4	Sisquoc Ranch (abd)	6	0	6	0	0	0	0
5	Zaca	31,792	1,836	33,628	4,206	0	4,206	125
6	Casmalia	43,608	1,584	45,192	18,818	157	18,975	420
7	Orcutt*	180,864	11,703	192,567	287,728	2,363	290,091	1,506
8	Four Deer (abd)	1,394	0	1,394	3,132	0	3,132	2,247
9	Harris Canyon Northwest (abd)	10	0	10	0	0	0	0
10	Careaga Canyon	439	0	439	797	0	797	1,815
11	Los Alamos	357	0	357	212	0	212	594
12	Barham Ranch	4,614	1,541	6,155	7,139	5,375	12,514	2,033
13	Jesus Maria	295	0	295	41	0	41	139
14	Lompoc*	48,449	1,543	49,992	47,498	2,659	50,157	1,003
			Total oil:	881,373		Total gas:	851,106	966
	*Cross section 12.14		Total BOE:	1,023,224				

Table 2. Table of known oil fields in the Santa Maria Basin. "Field No." refers to the number shown in bold next to each oil field in **Figure 11.** Mbbl, thousands of barrels; ER, expected recovery; MMCF, million cubic feet; GOR, gas-pol-ratio.

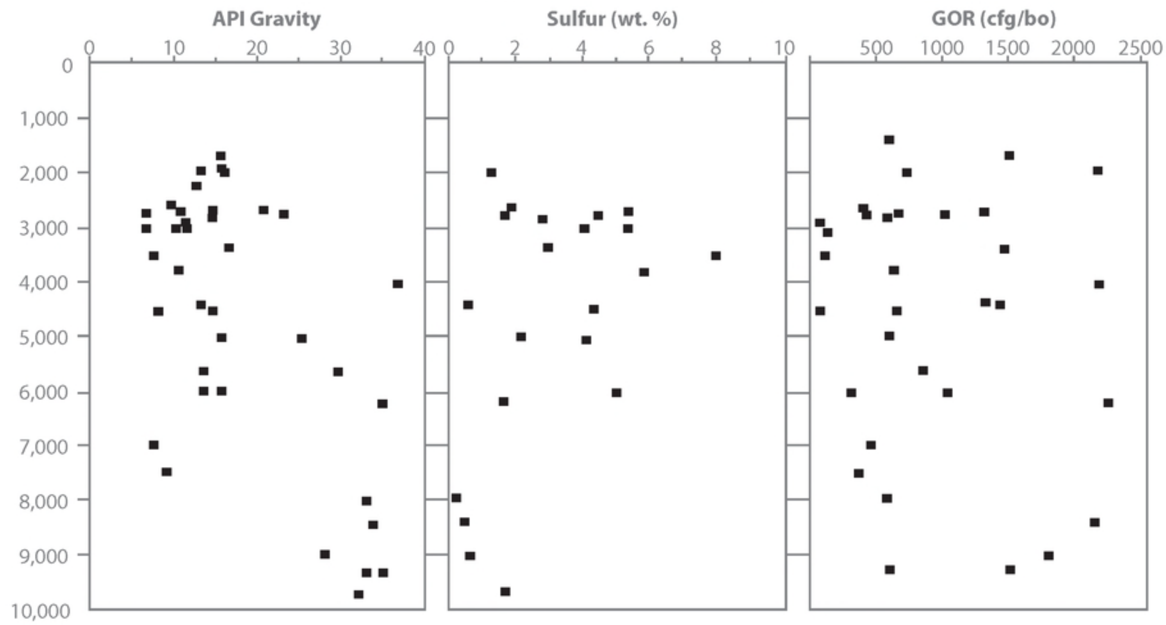

Figure 13. Bulk oil properties by pool vs. depth in the Santa Maria Basin. Data are from California Division of Oil, Gas, and Geothermal Resources (2010).

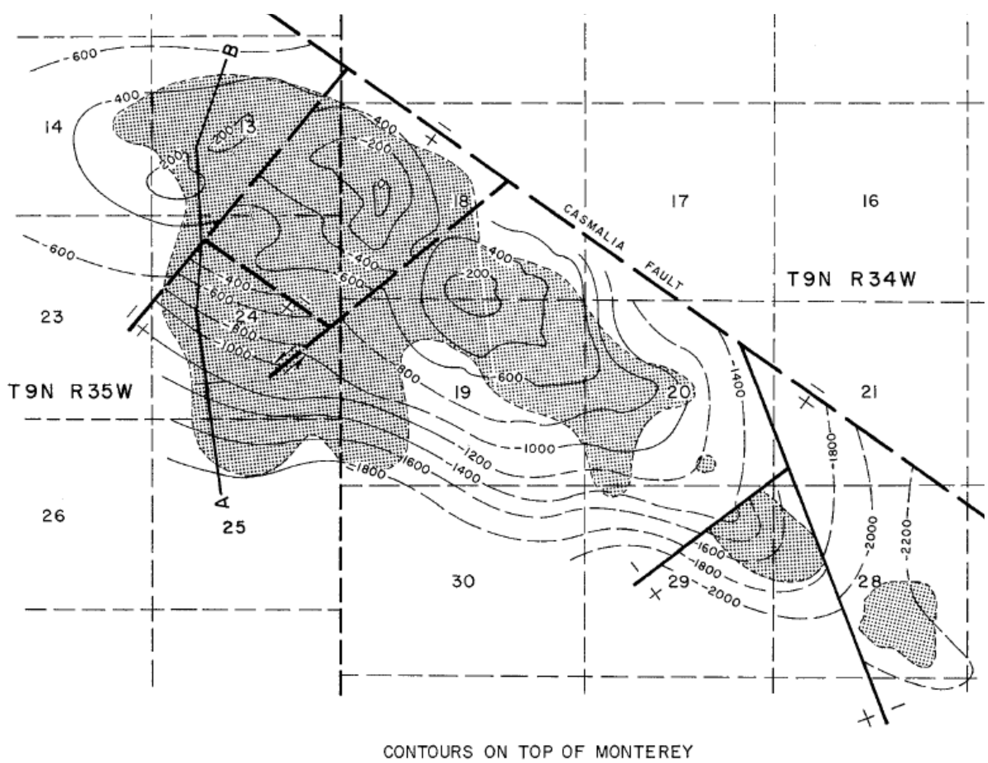

Figure 14. The oil-water contact in Casmalia field fail to follow structural depth contours of the Monterey Formation, indicating it is under-charged. Figure from California Division of Oil, Gas, and Geothermal Resources (1998).

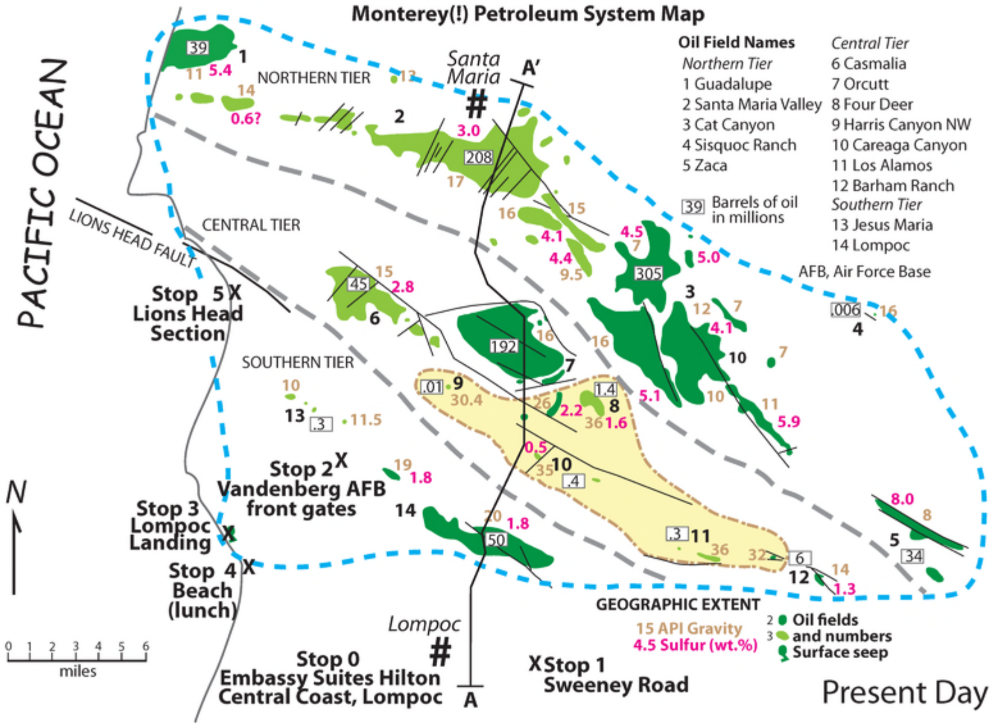

Figure 15. Map of the Monterey(!) petroleum system illustrating the weight (API gravity in light brown text) and sulfur content (pink text) of produced oil. The yellow shading denotes the region expelling oil between 15 and 35 API gravity oil, or what we propose is the native Monterey oil in this system.

Description of Individual Field Trip Stops

There are numerous excellent field trip guides to the outcrops of the Santa Maria Basin: Isaacs (1984), Dunham and Blake (1987), and Behl (2000) are just a few. In compiling this field guide, we have selected aspects of these publications that are relevant to the discussion of the petroleum system. We also add our interpretations of how each outcrop exemplifies the essential elements of the Monterey(!) petroleum system.

Stop 1: Sweeney Road

This first field trip stop in the Monterey(!) petroleum system lies near the southern margin of the Santa Maria Basin along the Santa Ynez River (**Figure 3**). Here we investigate the overburden rocks— late Miocene Monterey and late Miocene to early Pliocene Sisquoc Formation—that likely created sufficient thermal stress to push the Monterey source rock into the oil window (**Figure 16**). This road cut measures 1650 ft (500 m) long by 260 ft (80 m) high (Wirtz, 2017). The formational contact between the Monterey and Sisquoc formations is difficult to discern in the Sweeney Road outcrop because both units are highly biosiliceous and likely were deposited, at least at the scale of basinal-depth depositional troughs, in similar geologic conditions (Behl, 2000). The principal lithology encountered in this outcrop is interbedded laminated to massive diatomaceous mudstone in the opal-A phase (**Figure 17**) (Dumont and Barron, 1995). Variation in the composition of the original sediment influence the timing and burial depth of the silica phase change on a bed-by-bed basis creating distinct stratigraphic packages of porous and permeable diatomaceous rocks that alternate with relatively nonporous and brittle rocks (chert and porcelanite).

The large-scale interpretation by Wirtz (2017) of the stratigraphy exposed on Sweeney Road is shown in **Figure 18**. At the north end of the outcrop, we start in the basal Sisquoc Formation, a siliceous mudstone in the opal-A phase, indicating moderate depth and temperature of burial (**Figure 7**). In the ~1 m.y. of section exposed here (5 to 6 Ma; Dumont and Barron, 1995), the Sisquoc contains both laminated and massive intervals (Behl, 2000). Whereas the massive beds tend to be darker in color and extensively bioturbated (indicative of relatively more oxygenated bottom waters), the laminated beds, indicating relative anoxia, are also generally lighter-colored, purer diatomites (Behl, 2000). These diatomaceous sediments have high porosity of 50-75% (Rick Behl, personal communication).

As we walk south along Sweeney Road, we quickly encounter the Sisquoc-Monterey Formation boundary, which coincidentally falls at or near the top of the opal A-opal CT transition in this outcrop. Silica-rich sediments in this part of the upper, clayey-siliceous member of the Monterey Formation (6 to 8 Ma) occur as diatomite, porcelanite, and chert (Behl, 2000) The Monterey here is finely laminated, fractured, and deformed at a variety of scales (**Figure 19**).

Gross tectonic features exposed at Sweeney Road are an anticline-syncline pair with fold angles of 68° for the anticline and 98° for the syncline and steeply north-dipping axial planes (**Figure 18**) (Wirtz, 2017). Other structural styles include both harmonic and disharmonic folds and evidence of simple shear, pure shear, and flexural slip (**Figure 20**) (Wirtz, 2017). Gutiérrez-Alonso and Gross

(1997) characterize the folds at Sweeney Road as Group III folds, which are asymmetric with a dominant S-directed vergence (**Figure 21).**

Wirtz (2017) proposes that the observed mechanical stratigraphy in this outcrop is diagenetically controlled: less competent diatomaceous beds (predominant in the Sisquoc Formation) accommodate strain by horizontal compaction and gentle folding whereas more competent porcelaneous beds in the Monterey Formation accommodate strain with a variety of folding geometries. This is an excellent place to observe the complex structural geometries created by flexural slip folding so common in thinly bedded rocks like the Monterey Formation.

The tight folds seen at Sweeney Road are part of the broader Lompoc-Santa Rosa fold belt (Wirtz, 2017) and are an analog for subsurface structural traps in the Santa Maria Basin.

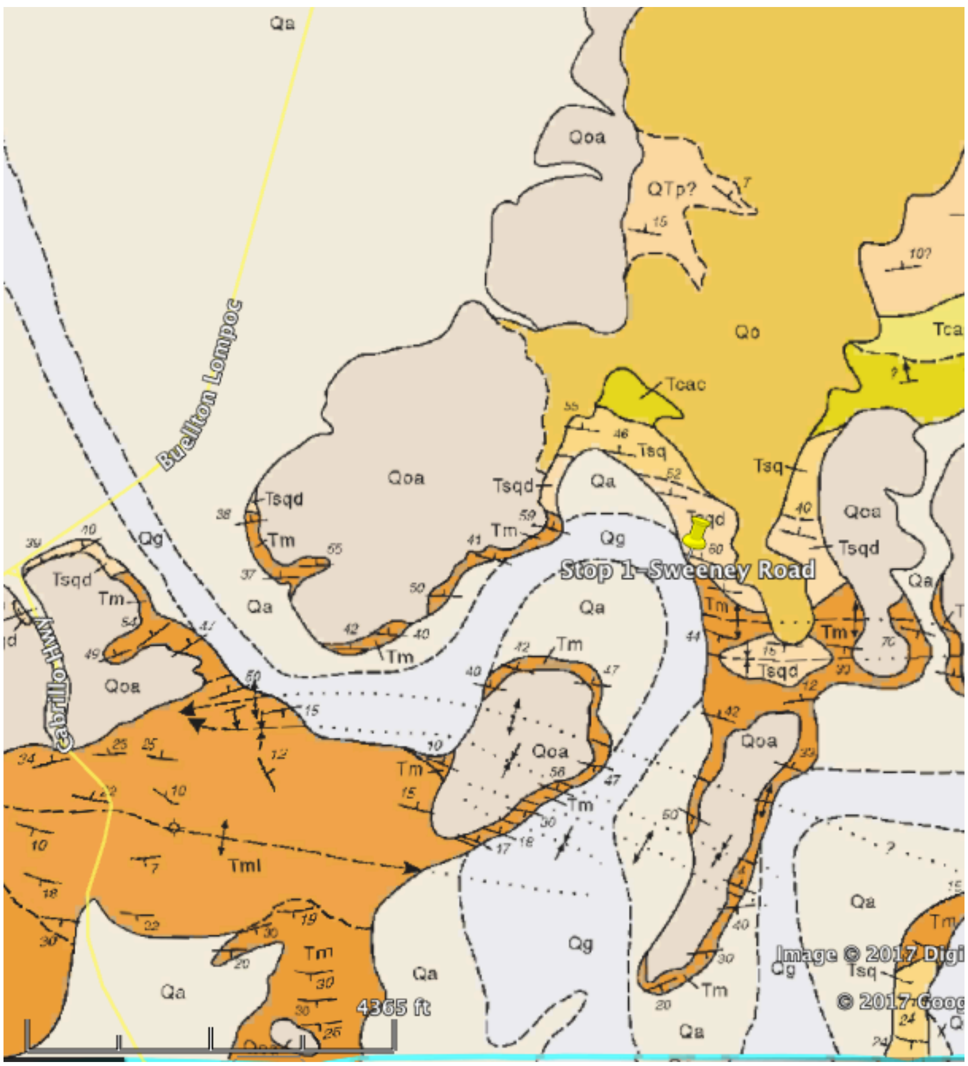

Figure 16. Geologic map of Sweeney Road from Dibblee (1950). Tsq, Sisquoc Formation; Tsqd, Sisquoc Formation diatomite; Tm, Monterey Formation; abbreviations starting with “Q” are Quaternary rocks.

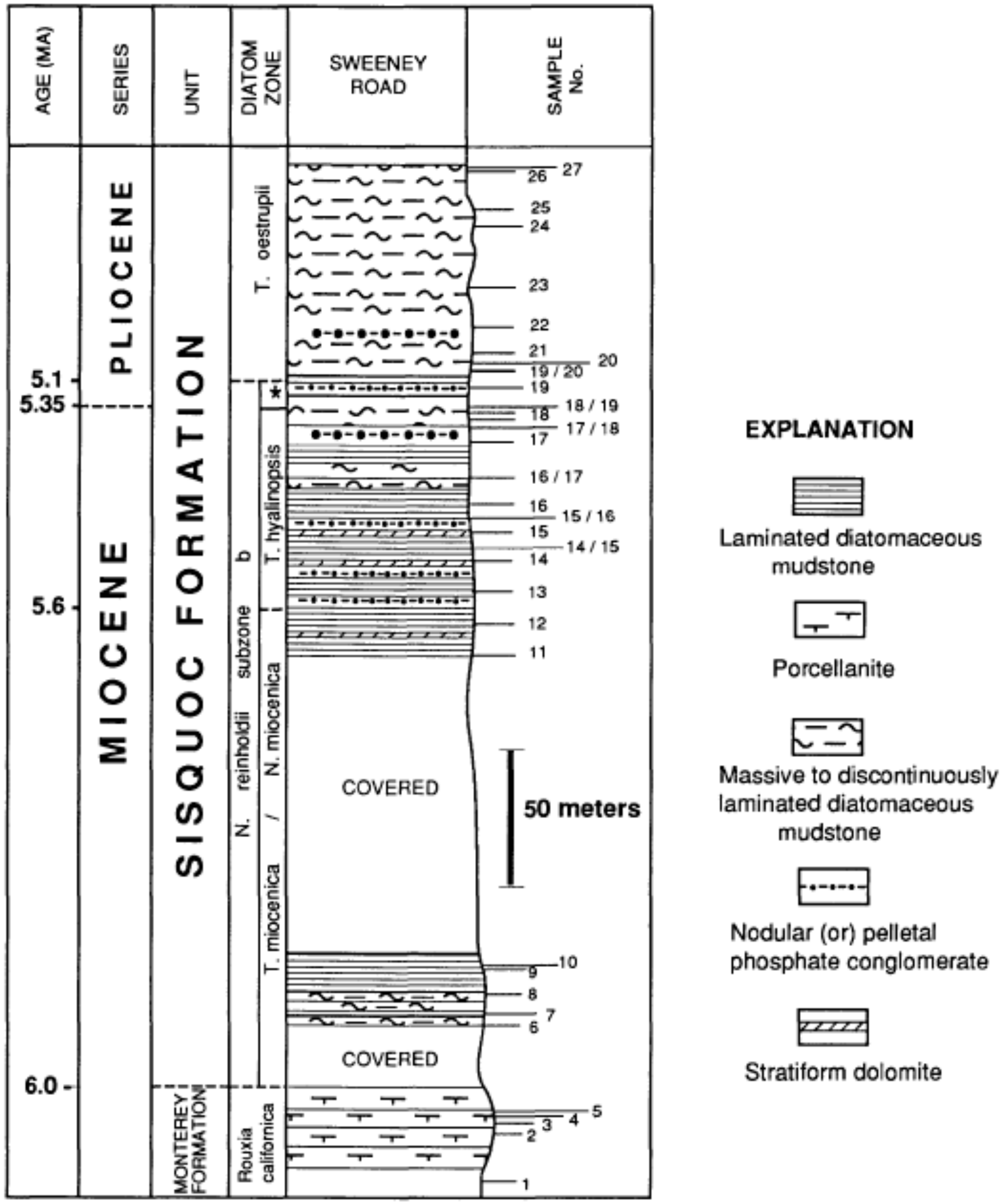

Figure 17. Detailed figure of lithologic stratigraphy in the Sisquoc exposed in the Sweeney Road outcrop (Dumont and Barron, 1995). Sample numbers refer to samples studied for biostratigraphy.

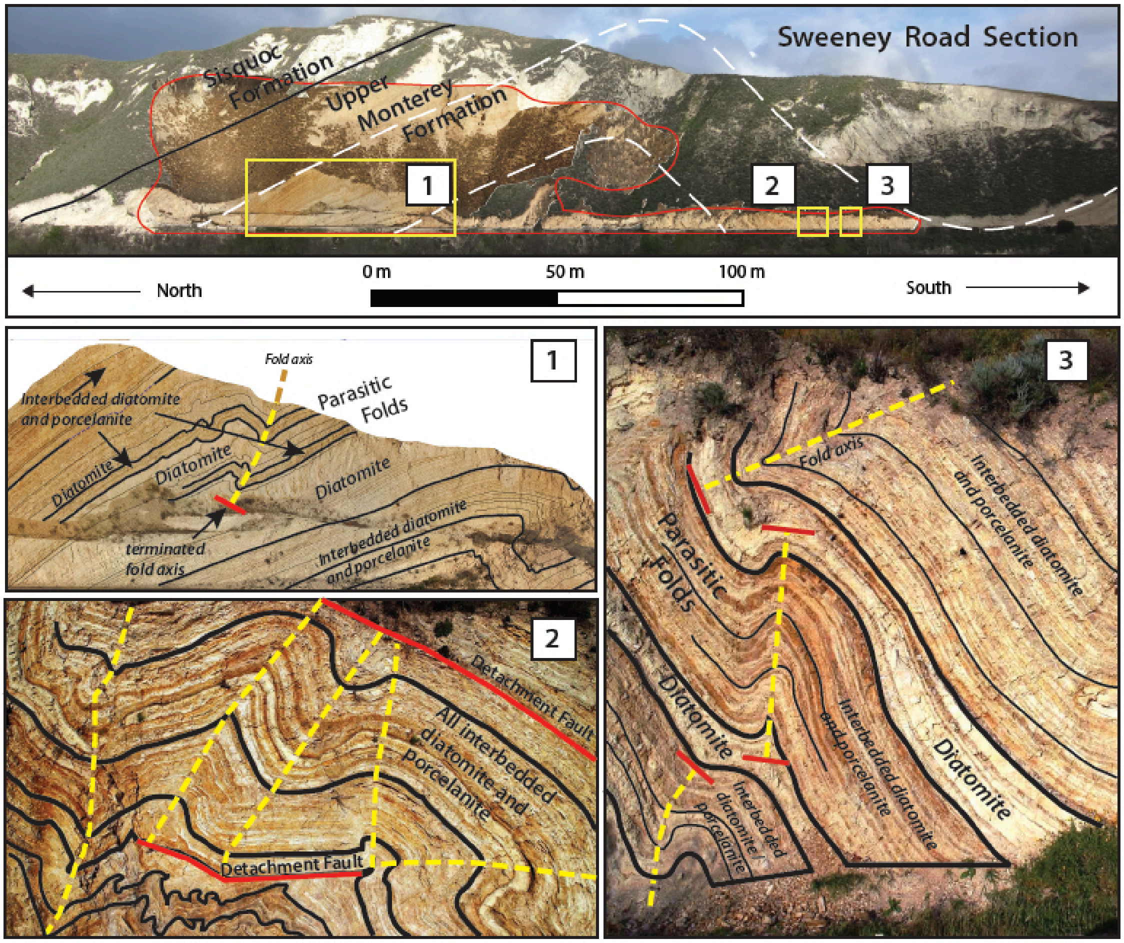

Figure 18. The basal Sisquoc Formation is exposed at the north end of the Sweeney Rd outcrop and is underlain by the upper Monterey Formation. Together the units form an anticline-syncline pair. Various styles of deformation are interpreted in boxes 1, 2, and 3. Figure from Wirtz (2017).

Figure 19 Photo detail down section (relative to previous photo) of Monterey Formation outcrop on Sweeney Road illustrating intricate folds.

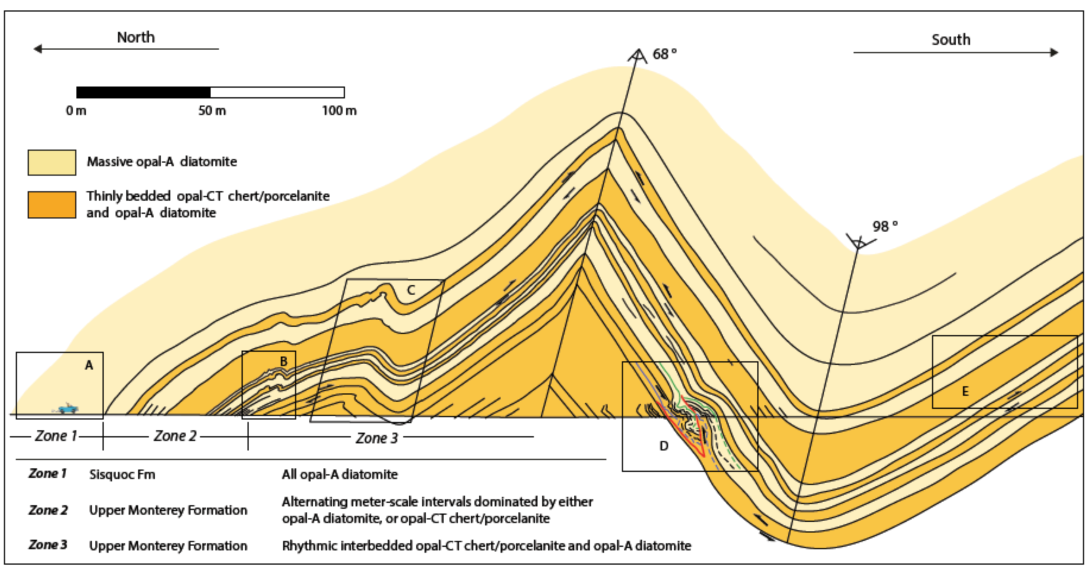

Figure 20. Interpretation by Wirtz of approximately 1300 ft (400 m) of the outcrop at Sweeney Rd. A, massive beds; Sisquoc Formation. B, disharmonic folds; C, harmonic folds; D, limb faults and buckle folds; E, pure flexural slip. B through E in the Monterey Formation.

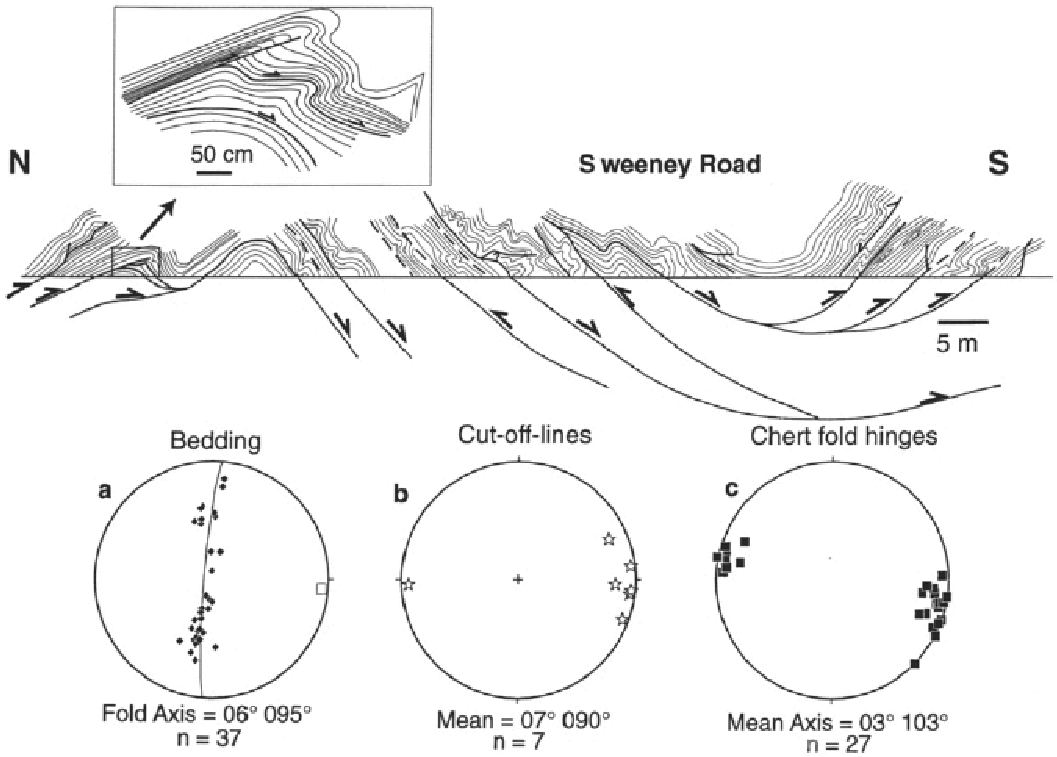

Figure 21. Structural data from the Sweeney Road outcrop mapped by Guitérrez-Alonso and Gross (1997). Stereonet a) Poles to bedding plotted on a π diagram; Stereonet b) thrust cutoff lines; Stereonet c) Group III fold hinges. Plotted orientation of smaller-scale chert/porcelanite folds are parallel to larger anticline-syncline axes, indicating contemporaneous formation.

Stop 2: Vandenberg Air Force Base Visitors' Center

Vandenberg Air Force Base covers 99,000 acres of California's central coast. Access to the base is restricted and visitors should pre-arrange a trip to the coastal outcrops with the Public Affairs Office. Some interesting facts about Vandenberg are:

- More than 10% of the land burned in a September 2016 wildfire.
- There are 17 endangered species on the base.
- There are ~2400 Chumash Indian archaeological sites ranging from rock art to shell mounds. The Chumash still have access to their spiritual sites through an agreement with the base.
- There are no airplanes at Vandenberg Air Force Base.
- A runway was extended to 3 miles length in 1985 for use as a west coast launch site for the Space Shuttle but its use was delayed following the loss of the Challenger and then its planned use was discontinued.
- Elon Musk is a frequent visitor to the base for SpaceX launches.

Stop 3: Lompoc Landing

The next stop on our "virtual drilling" tour of the Monterey(!) petroleum system is Lompoc Landing, a coastal outcrop of the upper calcareous-siliceous member of the Monterey Formation (**Figure 6**). The significance of this stop is the intensely fractured nature of the opal-CT and quartz phase rocks—a spectacular analog for the prolific subsurface reservoir rock in the Santa Maria Basin. Although we are in the same upper calcareous-siliceous member here that we'll see at the upper part of Lions Head, at Lompoc Landing the unit is caught within the opal-CT to quartz phase transition whereas at Lions Head it is entirely in the quartz phase. Thus, we can infer that at Lompoc Landing, the Monterey Formation was buried less deeply than its counterpart at Lions Head.

The outcrop at Lompoc Landing has been called an "exhumed oil field" because of the excellent examples of oil-filled fractures and asphalt-bearing breccia (Dunham and Blake, 1987). The absence of cement-filled fractures indicates that oil displaced water from the system before cementation occurred (Dunham and Blake, 1987), likely simultaneously with brittle deformation.

This outcrop occupies the broad crest of the Lompoc-Purisima Anticline, which extends for ~45 km inland from the coast (**Figure 3**). Beds are nearly flat lying, resulting in minimal structural relief (Gutiérrez-Alonso and Gross, 1997) (**Figures 22, 23**). The horizontal attitude of bedding at Lompoc Landing permits the examination of fractures and fracture patterns within the Monterey. These occur over a range of scales and morphologies.

Based on extensive field mapping, Finn et al. (2003) categorized these into four types: bed-confined joints, throughgoing joints, linked and open throughgoing joints, and breccia zone (**Figure 24**). Joints that are confined to beds have vertical to sub-vertical dips and occur in NW-SE (shorter cross joints) and NNE-SSW (longer systematic joints) directions (Finn et al., 2003). (**Figures 24, 25**). The systematic joints are part of a regional hinge-normal joint sets seen in outcrops throughout the basin (Finn et al., 2003).

Throughgoing fractures link the systematic and cross joints on the scale of meters to tens of meters and cut obliquely through the formation (Finn et al., 2003) (**Figures 24, 25**). When open, the throughgoing fractures have overall widths up to tens of centimeters with millimeter- to centimeter-scale open apertures. When filled with asphalt, their role as oil migration and storage agents in the petroleum system is clear. The final stage, the asphalt-breccia zone (**Figures 24**, **26**), links fractured layers across interbedded, non-fractured shales, providing crucial vertical hydraulic connectivity (MacKinnon, 1989). Because of the intensely fractured and brecciated nature of the upper calcareous member of the Monterey Formation as seen here at Lompoc Landing, its permeability is ten times or more that of the less fractured clayey-siliceous member (MacKinnon, 1989).

The Monterey Formation at Lompoc Landing also features brecciation and buckling of dark colored quartz chert layers within buff colored laminated opal-CT rock, resulting in "contorted chert." (**Figure 27**). Dunham and Blake (1987) explain that opal-CT chert beds fracture at scales smaller than bed scale, and that these individually fractured layers of just a few mm thickness shatter independently, resulting in very-small clasts that rotate individually during folding.

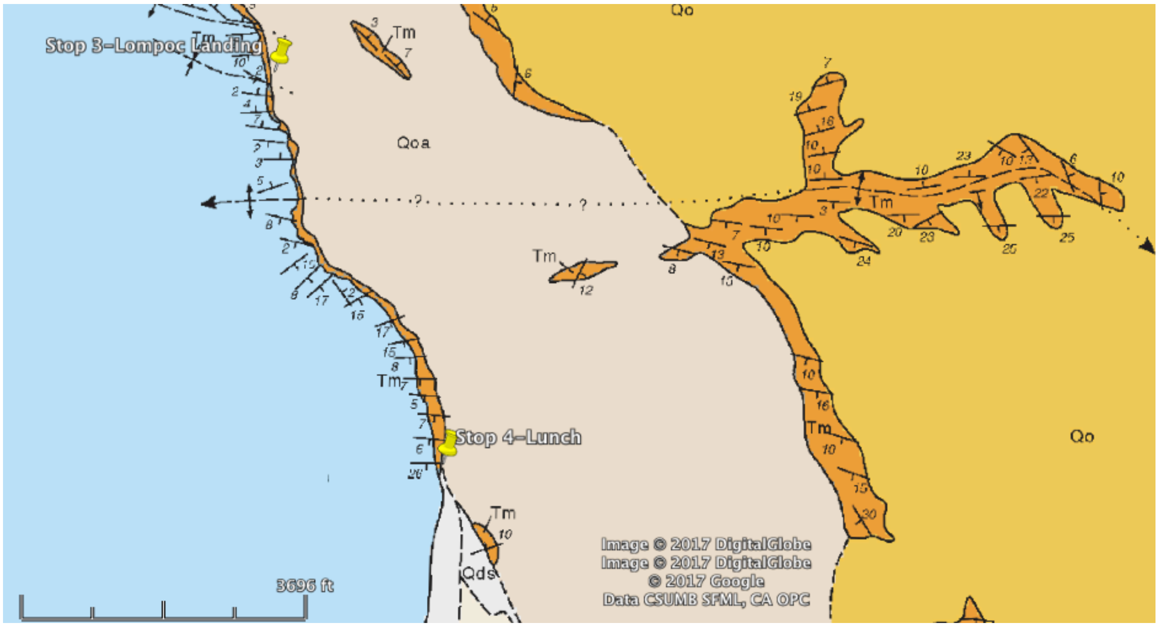

Figure 22. Geologic map of Lompoc Landing from Dibblee (1950). Tm, Monterey Formation; abbreviations starting with "Q" are Quaternary rocks. Dip measurements emphasize the gentle regional orientation of the sliver of Monterey exposed at the coast.

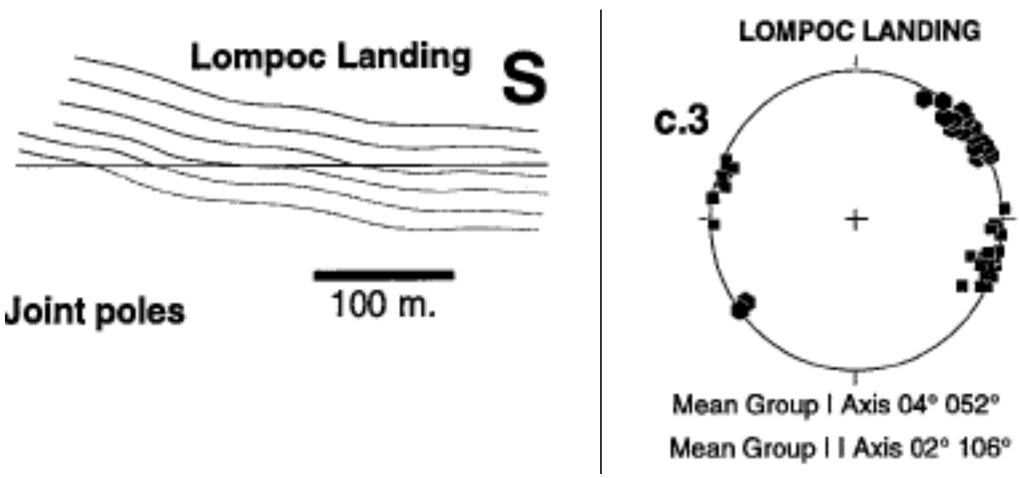

Figure 23. (Left) The nearly flat-lying beds of the upper Monterey Formation and (Right) Stereonet of Group I fold hinges, as mapped by Guitérrez-Alonso and Gross (1997).

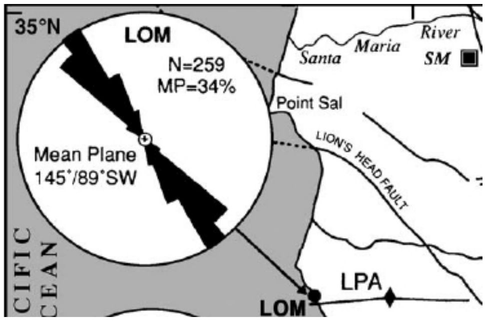

Figure 24. Structural analysis data at Lompoc Landing (LOM). (Top left) Kinematic data from linked, through going fractures. LPA, Lompoc-Purisima Anticline. (Middle) Conceptual model of four fracture morphologies. (Bottom) Stereoplots and rose diagrams of fracture data for systematic joints, cross joints, and throughgoing fractures. Figures from Finn et al (2003).

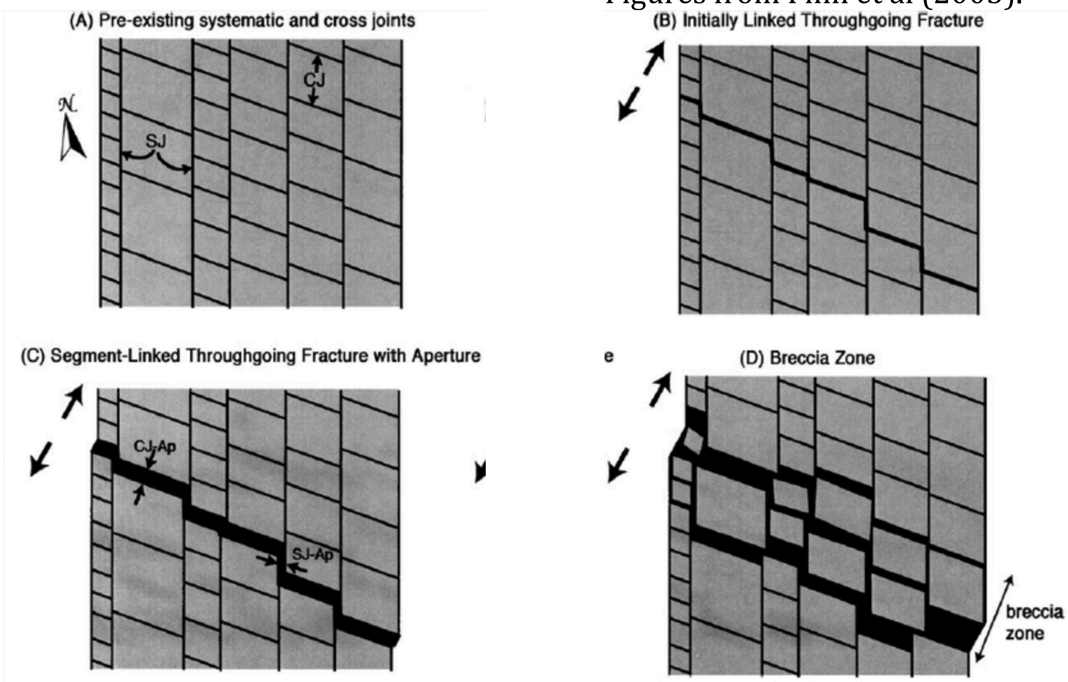

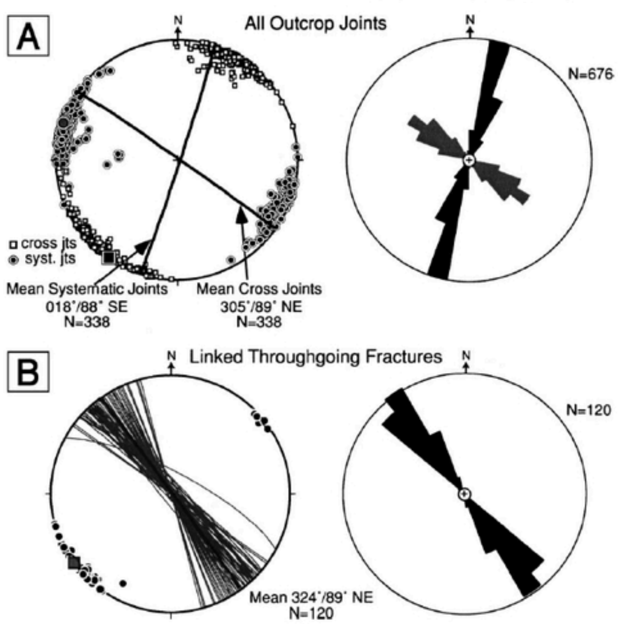

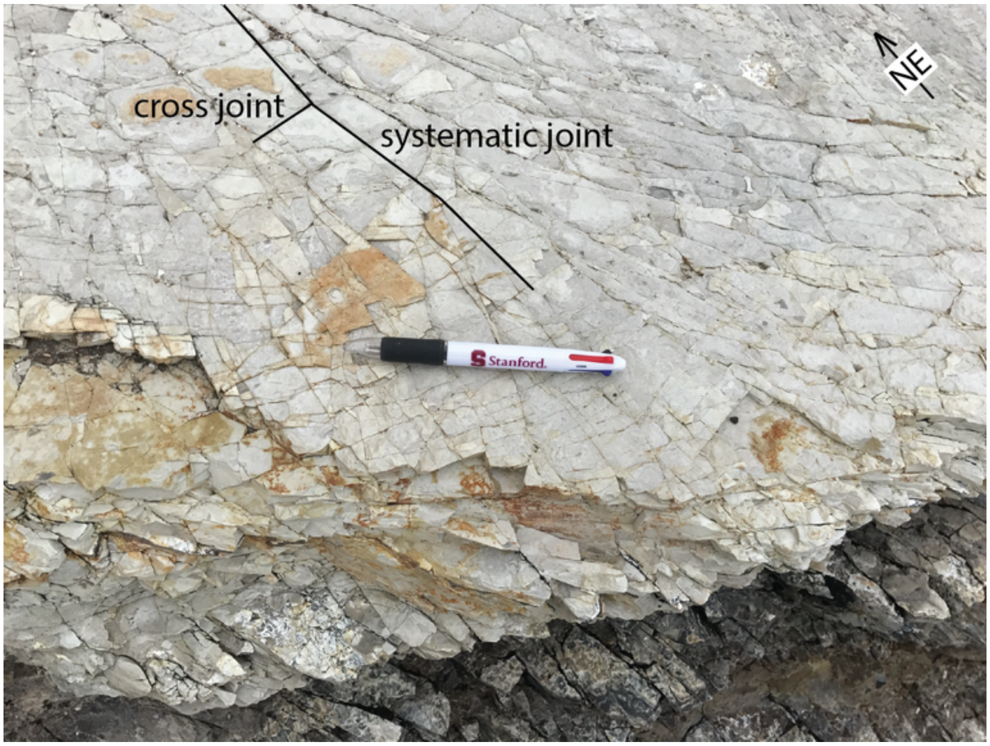

Figure 25. Photograph of systematic and cross joints, as defined and interpreted by Finn et al. (2003).


Figure 26. This photograph illustrates systematic joins, cross joints, thoroughgoing fractures, and asphalt filled breccia at Lompoc Landing.

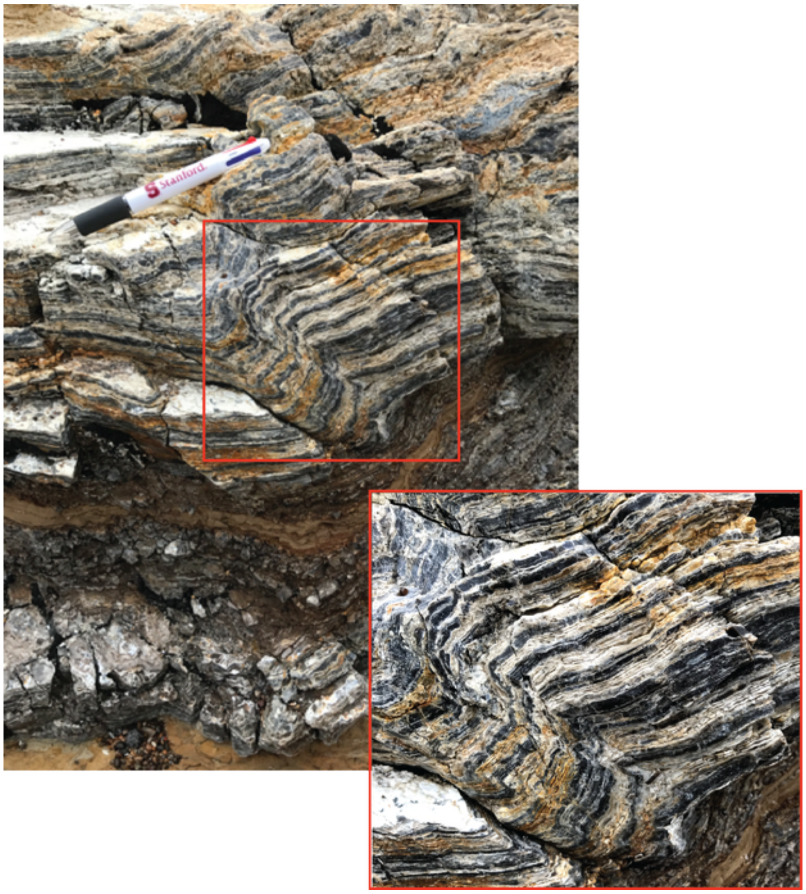

Figure 27. Highly contorted chert within the opal-CT phase upper Monterey at Lompoc Landing.

Stop 4: Beach lunch stop

Stop 5: Lions Head

The Monterey section at Lions Head beach is probably the best-studied outcrop in all of the Santa Maria Basin. This final field trip stop takes advantage of an exposure of the lower Monterey Formation where it is in contact with the Point Sal Ophiolite across the Lions Head Fault, a ~100 m.y. nonconformity (**Figure 28**). After carefully scrambling down the rocks to the beach, turn right/walk north to the contact between the Monterey and the ophiolite (**Figure 29**). We will then turn around and walk south, or upsection, through the Monterey.

Lithology

All of the ~1000 ft (305 m) of (almost entirely) exposed vertical section of Monterey Formation is in the quartz diagenetic grade of silica at Lions Head. This include the sparse diagenetic silica in the organic-rich mudstones, dolomites, etc. "Typical" clay-bearing quartz-phase rocks like porcelanite or siliceous mudstone, require a phase transformation temperature of between about 70°C and 90°C (**Figure 7**). However, the cherts near the top of the exposed section initially formed in the opal-CT phase within a few hundred meters of burial and with as little as 15 to 20°C of burial-related heating; conversion to quartz-phase chert occurred tens of degrees and hundreds of meters shallower than typically occurs in less siliceous lithologies (Behl, 2000; Behl and Garrison, 1994). This "early" formation of hard, brittle rocks within otherwise still weak and porous sediments has a profound influence on the style of deformation and on fluid flow through fractured rocks.

The base of the Monterey Formation above the Lions Head Fault is uppermost Relizian-Luisian in age and comprises clay mudstone and dolomite. The lower section is mostly part of the phosphatic shale member (**Figure 6**) (Dunham and Blake, 1987). Deformation associated with the fault extends about 80 feet (25 m) into the Monterey. Dunham and Blake (1987) suggest that most of the lower Monterey Formation is preserved at the Lions Head Fault; their evidence is the presence of thin sand layers, interpreted as turbidites, that have their source in the Point Sal Formation, which underlies the Monterey in other parts of the basin.

This lower part of the Monterey Formation is phosphatic, organic-rich, calcareous, and siliceous (Behl, 2000). A dramatic feature in this section of the Monterey are laterally persistent dolostone beds, tan to orange in color, that variously comprise 10 to 50% of the section (Behl, 2000) (**Figure 30**). These brittle, low porosity dolostone beds are the key to biostratigraphic dating of this part of the Monterey, as they enclose preserved diatoms (MacKinnon, 1989). The dolostone beds are encased within phosphatic shale and phosphatic marlstone, which themselves exhibit a variety of geometries including laminations and lenses (lower) and massive beds (upper) (**PHOTO 31**).

The upper calcareous-siliceous middle member of the Monterey Formation overlies the phosphatic member (**Figure 6**). It is lithologically heterogeneous but is distinguished at Lions Head by an abundance of chert, essentially preserving a record of pure biogenic silica ooze (Behl, 2000). Deposition of the chert facies began in the Santa Maria basin about 12.9 Ma (Behl, 2000; White et al., 1992). Of particular note in this section of the Monterey are tightly buckled and brecciated sections and interbedded thin laminations of dark quartz cherts with light-colored opal-CT cherts, also called "tiger-stripe chert" (**Figure 32**). The quartz-phase chert fracture as described above for Lompoc Landing.

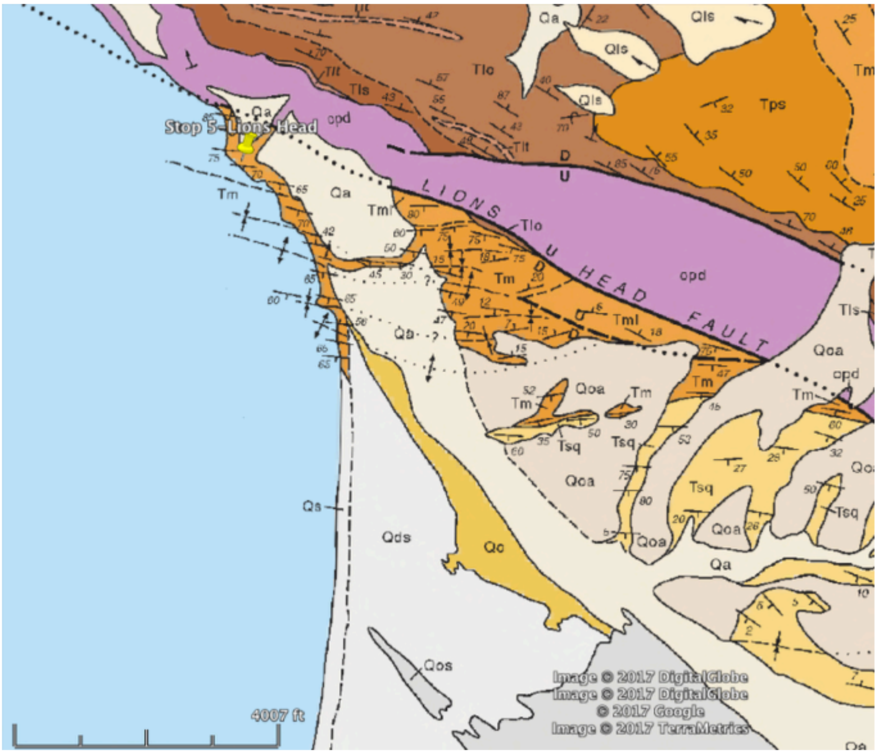

Figure 28. Geologic map of Lions Head from Dibblee (1950). Tm, Monterey Formation; Tml, lower Monterey Formation; Tsq, Sisquoc Formation; Tps, Point Sal Formation; opd, Coast Range ophiolite; abbreviations starting with "Q" are Quaternary rocks.

Figure 29. The Point Sal Ophiolite consists of serpentinized ultramafic rocks. Volcanic and plutonic cobbles and boulders from the ophiolite suite are on the beach.

Figure 30. Dolostone (tan to orange resistive beds) form laterally extensive layers interbedded with phosphatic mudstone in the lower Monterey Formation at Lions Head.

Figure 31. Thin, white lenses and laminations are likely phosphate of the lower Monterey Formation at Lions Head. Bottom, "tiger-striped cherts" consisting of alternating dark quartz-phase chert and light opal-CT chert or dolomite.

Figure 32. Contorted, buckled quartz-phase chert in the upper calcareous-siliceous member of the Monterey Formation.

Structure

A sketch and structural data for beds and folds of the Monterey Formation at Lions Head is shown in **Figure 33**. Beds are moderate to vertically dipping and the regional fold axis is mapped at 06°/098° is defined from combining outcrop data from across the region (Gutiérrez-Alonso and Gross, 1997). Faults and folds at Lions Head record episodes of Miocene extension and inversion.

Deformational styles of the Monterey at Lions Head are dependent on lithology. MacKinnon (1989) found fracture spacing at Lions Head to be smallest in chert at 0.6 cm and largest in dolostone at 6.6 cm, with porcelanite (2.5 cm) and mudstone (5.5) cm in between. Gross (1995) determined that "strong" lithologies—those with a small percentage of weak minerals—fail by opening mode fracture whereas "weak" lithologies (>~20% weak minerals) fail by faulting. In other words, faults develop in mudstone and mode I fractures form in dolostone.

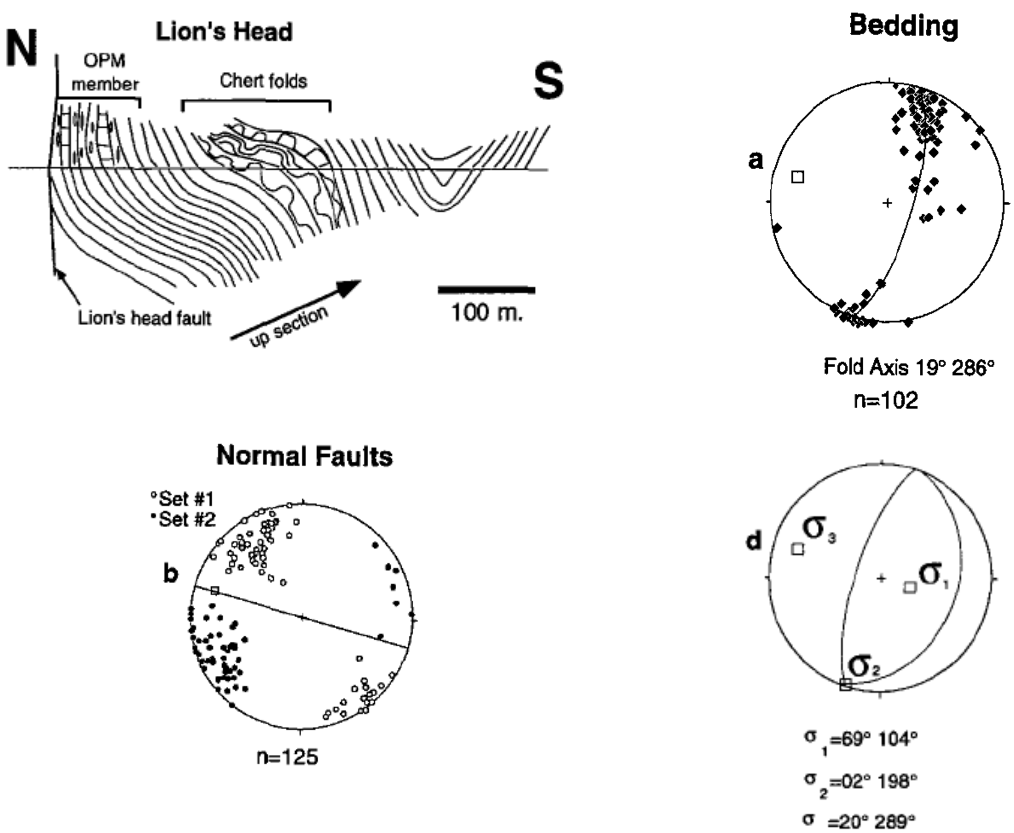

Figure 33. Structural data from Gutiérrez-Alonso and Gross (1997) for the Monterey Formation at Lions Head. Stereonets of a) bedding plane with mean fold axis, b) poles of conjugate populations of normal faults, and d) principal stress directions.

Geochemisty

Extensive geochemical profiling of the Monterey source rock at Lions Head was performed as part of the Cooperative Monterey Organic Geochemistry Study (CMOGS) and compiled in a landmark volume edited by Isaacs and Rullkötter (2001). We discuss much of this in the source rock section above, but in summary, all but 3 of 34 samples taken over 900 vertical feet of section (275 m) are type I kerogen with greater than 2 weight % organic carbon. All geochemical indicators show that the Monterey at Lions Head is thermally immature for oil generation, but we can use the degree of silica diagenesis to estimate how deeply it was buried prior to uplift.

References

Arnold, R., and R. Anderson, 1907, Preliminary report on the Santa Maria oil district, Santa Barbara County, California, Washington, U.S. Geological Survey Bulletin No. 317, p. 69.

Behl, R. J., 2000, Field guide to the geology of the Neogene Santa Maria Basin—From rift to uplift: Los Angeles, The Pacific Section SEPM (Society for Sedimentary Geology), 56 p.

Behl, R. J., and R. E. Garrison, 1994, The origin of chert in the Monterey Formation of California (USA), *in* A. Iijima, A. Abed, and R. E. Garrison, eds., Siliceous, phosphatic, and glauconitic sediments of the Tertiary and Mesozoic: Proceedings of the 29th International Geologic Congress, Part C: Utrecht, VSP, p. 101-132.

CA DOGGR, 2010, 2009 Annual Report of the State Oil and Gas Supervisor, Sacramento, Calif., California Department of Conservation, Division of Oil, Gas, and Geothermal Resources, p. 267.

CDOGGR, 1998, California oil and gas fields: Sacramento, Calif., California Department of Conservation, Division of Oil, Gas, and Geothermal Resources Publication No. CD-1, 1472 p.

CDOGGR, 2010, 2009 Annual Report of the State Oil and Gas Supervisor, Sacramento, Calif., California Department of Conservation, Division of Oil, Gas, and Geothermal Resources Publication No PR06,, p. 267.

Curiale, J. A., D. Cameron, and D. V. Davis, 1985, Biological marker distribution and significance in oils and rocks of the Monterey Formation, California: Geochimica et Cosmochimica Acta, v. 49, p. 271-288.

Dibblee, T. W., Jr., 1950, Geology of southwestern Santa Barbara County, California: Point Arguello, Lompoc, Point Conception, Los Olivos, and Gaviota quadrangle (1:62,500): California Division of Mines and Geology Bulletin 150.

Dickinson, W. R., M. N. Ducea, L. I. Rosenberg, H. G. Greene, S. A. Graham, J. C. Clark, G. E. Weber, S. Kidder, W. G. Ernst, and E. E. Brabb, 2005, Net dextral slip, Neogene San Gregorio-Hosgri fault zone, coastal California—Geologic evidence and tectonic implications: Geological Society of America Special Paper, v. 391, p. 1-43.

Dralus, D., 2013, Chemical interactions between silicates and their pore fluids: How they affect rock physics properties from atomic to reservoir scales: Doctoral thesis, Stanford University, Stanford, CA, 153 p.

Dumont, M. P., and J. A. Barron, 1995, Diatom biochronology of the Sisquoc Formation in the Santa Maria Basin, California, and its paleooceanographic and tectonic implications, *in* M. A. Keller, ed., Evolution of sedimentary basins/onshore oil and gas investigations—Santa Maria Province: Reston, Va., U. S. Geological Survey Bulletin 1995—K, U. S. Geological Survey, p. K1-K17.

Dunham, J. B., and G. H. Blake, 1987, Guide to coastal outcrops of the Monterey Formation of western Santa Barbara County, California: Los Angeles, The Pacific Section, Society of Economic Paleontologists and Mineralogists, 36 p.

Dunham, J. B., and M. L. Cotton-Thorton, 1990, Lithology of the Monterey Formation in the western Santa Maria Valley field, Santa Maria Basin, California, *in* M. A. Keller, and M. K. McGowan, eds., Miocene and Oilgocene petroleum reservoirs of the Santa Maria and Santa Barbara-Ventura Basins, California—A core workshop: Tulsa, Okla., SEPM Core Workshop No. 14, June 3, 1990, p. 203-244.

Finn, M. D., M. R. Gross, Y. Eyal, and G. Draper, 2003, Kinematics of throughgoing fractures in jointed rocks: Tectonophysics, v. 376, p. 151-166.

Gross, M. R., 1995, Fracture partitioning: Failure mode as a function of lithology in the Monterey Formation of coastal California: GSA Bulletin, v. 107, p. 779-792.

Gutiérrez-Alonso, G., and M. R. Gross, 1997, Geometry of invertged faults and related folds in the Monterey Formation: Implications for the structural evolution of the southern Santa Maria Basin, California: Journal of Structural Geology, v. 19, p. 1303-1321.

Henderson, N. C., Jr.,, 1990, Control exerted by lithologic variations and pebbly units on petroleum occurrences in the Pliocene upper Sisquoc Formation, Casmalia Hills, Santa Maria Basin, California, *in* M. A. Keller, and M. K. McGowan, eds., Miocene and Oilgocene petroleum reservoirs of the Santa Maria and Santa Barbara-Ventura Basins, California—A core workshop: Tulsa, Okla., SEPM Core Workshop No. 14, June 3, 1990, p. 339-400.

Holditch, S. A., 2006, Tight gas sands: Journal of Petroleum Technology, v. 58, p. 86-93.

Ingle, J. C., Jr., 1981, Origin of Neogene diatomites around the Pacific North Rim, in R. E. Garrison, ed., The Monterey Formation and related siliceous rocks of California, *in* R. E. Garrison, and R. G. Douglas, eds., The Monterey Formation and related siliceous rocks of California: Los Angeles, Pacific Section, Society of Economic Paleontologists and Mineralogists, p. 159-179.

Isaacs, C. M., 1981a, Field trip guide for the Monterey Formation, Santa Barbara Coast, California, *in* C. M. Isaacs, ed., Guide to the Monterey Formation in the California coastal area, Ventura to San Luis Obispo, v. 52, Pacific Section, American Association of Petroleum Geologists, v. 52, p. 55-71.

Isaacs, C. M., 1981b, Lithostratigraphy of the Monterey Formation, Goleta to Point Conception, Santa Barbara coast, California, *in* C. M. Isaacs, ed., Guide to the Monterey Formation in the California coastal area, Ventura to San Luis Obispo, v. 52, Pacific Section, American Association of Petroleum Geologists, v. 52, p. 9-23.

Isaacs, C. M., 1981c, Outline of diagenesis in the Monterey Formation examined laterally along the Santa Barbara coast, California, *in* C. M. Isaacs, ed., Guide to the Monterey Formation in the California coastal area, Ventura to San Luis Obispo, v. 52, Pacific Section, American Association of Petroleum Geologists, v. 52, p. 25-38.

Isaacs, C. M., 1984, Field trip guide to deposition and diagenesis of the Monterey Formation, Santa Barbara and Santa Maria areas, California: U.S. Geological Survey Open File Report 84-98, p. 61.

Isaacs, C. M., 1992, Geology handbook for the Cooperative Monterey Organic Geochemistry Study, Santa Maria and Santa Barbara-Ventura basins, California: U.S. Geological Survey Open File Report 92-539-E, p. 1-35.

Isaacs, C. M., 2001, Depositional framework of the Monterey Formation, California, *in* C. M. Isaacs, and J. Rullkötter, eds., The Monterey Formation—From rocks to molecules: New York, Columbia University Press, p. 1-30.

Isaacs, C. M., and J. Rullkötter, 2001, The Monterey Formation—From rocks to molecules: New York, Columbia University Press, 553 p.

Isaacs, C. M., and J. H. Tomson, 1990, Reconnaissance study of petroleum source-rock characteristics of core samples from the Sisquoc and Monterey formations in a North-South subsurface transect across the onshore Santa Maria Basin and in surface sections along the Santa Barbara-Ventura coast, Southern California: Menlo Park, Calif., U.S. Geological Survey Open File Report 89-108, 43 p.

Jarvie, D. M., and L. L. Lundell, 2001, Kerogen type and thermal transformation of organic matter in the Miocene Monterey Formation, *in* C. M. Isaacs, and J. Rullkötter, eds., The Monterey Formation—From rocks to molecules: New York, Columbia University Press, p. 268-295.

Katz, B. J., and R. A. Royle, 2001, Variability of source rock attributes in the Monterey Formation, California, *in* C. M. Isaacs, and J. Rullkötter, eds., The Monterey Formation—From rocks to molecules: New York, Columbia University Press, p. 107-130.

Keller, M. A., 1990, Introduction to stratigraphy and hydrocarbon occurrence in Oilgocene and Miocene rocks of the Santa Barbara-Ventura and Santa Maria basins of California, *in* M. A. Keller, and M. K. McGowan, eds., Miocene and Oilgocene petroleum reservoirs of the Santa Maria and Santa Barbara-Ventura Basins, California—A core workshop: Tulsa, Okla., SEPM Core Workshop No. 14, June 3, 1990, p. 1-12.

Keller, M. A., and C. M. Isaacs, 1985, An evaluation of temperature scales for silica diagenesis in diatomaceous sequences including a new approach based on the Miocene Monterey Formation, California: Geo-Marine Letters, v. 5, p. 31-35.

Lillis, P. G., and L. B. Magoon, 2007, Petroleum systems of the San Joaquin Basin Province—Geochemical characteristics of oil types, *in* A. Hosford Scheirer, ed., Petroleum systems and geologic assessment of oil and gas in the San Joaquin Basin Province, California, U.S. Geological Survey Professional Paper 1713, chapter 9, p. 1-52 [available at http://pubs.usgs.gov/pp/pp1713].

MacKinnon, T. C., 1989, Petroleum geology of the Miocene Monterey Formation in the Santa Maria and Santa Barbara coastal and offshore areas, *in* T. MacKinnon, J. W. Randall, and R. E. Garrison, eds., Oil in the California Monterey Formation, Los Angeles to Santa Maria, California, July 20-24, 1989: Washington, D.C., American Geophysical Union Field Trip Guidebook T311, p. 11-27.

Magoon, L. B., and W. G. Dow, 1994, The petroleum system, *in* L. B. Magoon, and W. G. Dow, eds., The petroleum system—From source to trap, v. Memoir 60: Tulsa, Okla., American Association of Petroleum Geologists Memoir 60, p. 3-24.

McCrory, P. A., D. S. Wilson, J. C. Ingle, Jr., and R. G. Stanley, 1995, Neogene geohistory analysis of Santa Maria Basin, California, and its relationship to transfer of Central California to the Pacific Plate, *in* M. A. Keller, ed., Evolution of sedimentary basins/onshore oil and gas investigations—Santa Maria Province: Reston, Va., U. S. Geological Survey Bulletin 1995—J, U. S. Geological Survey, p. J1-J38.

Michael, G. E., 2001, Geochemical characterization of the Miocene Monterey Formation and oils in the Santa Barbara-Ventura and Santa Maria basins, *in* C. M. Isaacs, and J. Rullkötter, eds., The Monterey Formation—From rocks to molecules: New York, Columbia University Press, p. 241-267.

Namson, J., and T. L. Davis, 1990, Late Cenozoic fold and thrust belt of the southern Coast Ranges and Santa Maria Basin, California: The American Association of Petroleum Geologists Bulletin, v. 74, p. 467-492.

NOAA, 2017, Coastal Relief Model, https://maps.ngdc.noaa.gov/viewers/wcs-client/.

Orr, W. L., 2001, Evaluating kerogen sulfur content from crude oil properties—Cooperative Monterey organic geochemistry study, *in* C. M. Isaacs, and J. Rullkötter, eds., The Monterey Formation—From rocks to molecules: New York, Columbia University Press, p. 348-367.

Pelet, R., 1987, A model of organic sedimentation on present-day continental margins, *in* J. Brooks, and A. J. Fleet, eds., Marine petroleum source rocks: Oxford, Geological Society Special Publications No. 26, Blackwell Scientific Publications, p. 167-180.

Peters, K. E., and M. R. Cassa, 1994, Applied source rock geochemistry, *in* L. B. Magoon, and W. G. Dow, eds., The petroleum system—From source to trap: Tulsa, Okla., American Association of Petroleum Geologists Memoir 60, p. 93-117.

Peters, K. E., C. C. Walters, and J. M. Moldowan, 2005, The biomarker guide: Cambridge, U.K., Cambridge University Press, 1155 p.

Pisciotto, K. A., and R. E. Garrison, 1981, Lithofacies and depositional environments of the Monterey Formation, California, *in* R. E. Garrison, and R. G. Douglas, eds., The Monterey Formation and related siliceous rocks of California: Los Angeles, Pacific Section, Society of Economic Paleontologists and Mineralogists, p. 97-122.

Ramirez, P. C., and R. E. Garrison, 1995, Stratigraphy of the fine-grained facies of the Sisquoc Formation, Santa Maria Basin, California—Paleooceanographic and tectonic implications, *in* M. A. Keller, ed., Evolution of sedimentary basins/onshore oil and gas investigations—Santa Maria Province: Reston, Va., U. S. Geological Survey Bulletin 1995—U, U. S. Geological Survey, p. U1-U15.

Snyder, W. S., H. K. Brueckner, and R. A. Schweickert, 1983, Deformational styles in the Monterey Formation and other siliceous sedimentary rocks, *in* C. M. Isaacs, and R. E. Garrison, eds., Petroleum generation and occurrence in the

Miocene Monterey Formation, California: Los Angeles, Pacific Section, Society of Economic Paleontologists and Mineralogists, p. 151-170.

Stanley, R. G., S. Y. Johnson, C. C. Swisher, III, M. A. Mason, J. D. Obradovich, M. L. Cotton, M. V. Filewicz, and D. R. Vork, 1995, Age of the Lopse Formation (early Miocene) and origin of the Santa Maria Basin, California, *in* M. A. Keller, ed., Evolution of sedimentary basins/onshore oil and gas investigations—Santa Maria Province: Reston, Va., U. S. Geological Survey Bulletin 1995—J, U. S. Geological Survey, p. M1-M37.

Sweetkind, D. S., M. E. Tennyson, V. E. Langenheim, and L. E. Shumaker, 2010, Digital tabulation of stratigraphic data from oil and gas wells in the Santa Maria Basin and surrounding areas, central California coast, U.S. Geological Survey, p. 11.

Tennyson, M. E., and C. M. Isaacs, 2001, Geologic setting and petroleum geology of Santa Maria and Santa Barbara basins, coastal California, *in* C. M. Isaacs, and J. Rullkötter, eds., The Monterey Formation—From rocks to molecules: New York, Columbia University Press, p. 206-229.

U.S. Geological Survey, 2017, USGS Quaternary Fault and Fold Database, http://earthquake.usgs.gov/hazards/qfaults/.

White, L. D., R. E. Garrison, and J. A. Barron, 1992, Miocene intensification of upwelling along the California margin as recorded in siliceous facies of the Monterey Formation and offshore DSDP sites, *in* C. P. Summerhayes, W. L. Prell, and K.-C. Emeis, eds., Upwelling systems; evolution since the early Miocene: Geological Society Special Publication 64: Oxford, U.K., Blackwell, p. 429-442.

Wilson, D. S., P. A. McCrory, and R. G. Stanley, 2005, Implications of volcanism in coastal California for the Neogene deformation history of western North America: Tectonics, v. 24, p. 22.

Wirtz, Y., 2017, Strain variation between the Monterey and Sisquoc formations, Southern Santa Maria Basin, California, USA: Implications for structural assessment of fold and thrust belts: Masters thesis, California State University, Long Beach, Long Beach, 78 p.

Notes

Notes